

# UNIVERSITY OF TWENTE.

Faculty of Electrical Engineering, Mathematics & Computer Science

# Markers of Brain Resilience

Anubrata Bhowmick
M.Sc. Final Thesis July, 2021
in collaboration with



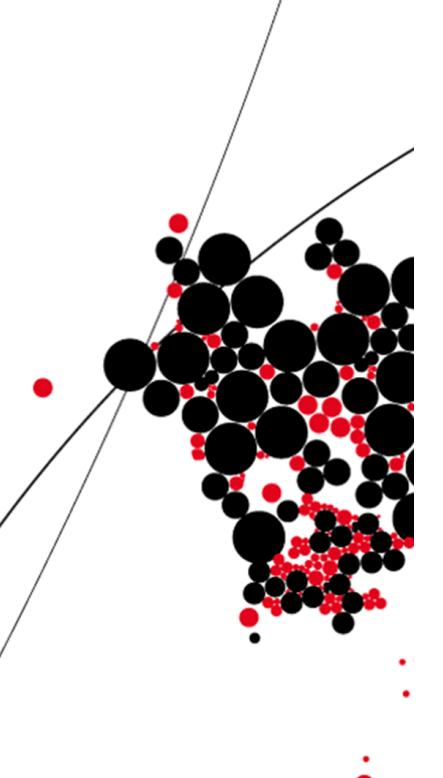
#### Supervisors:

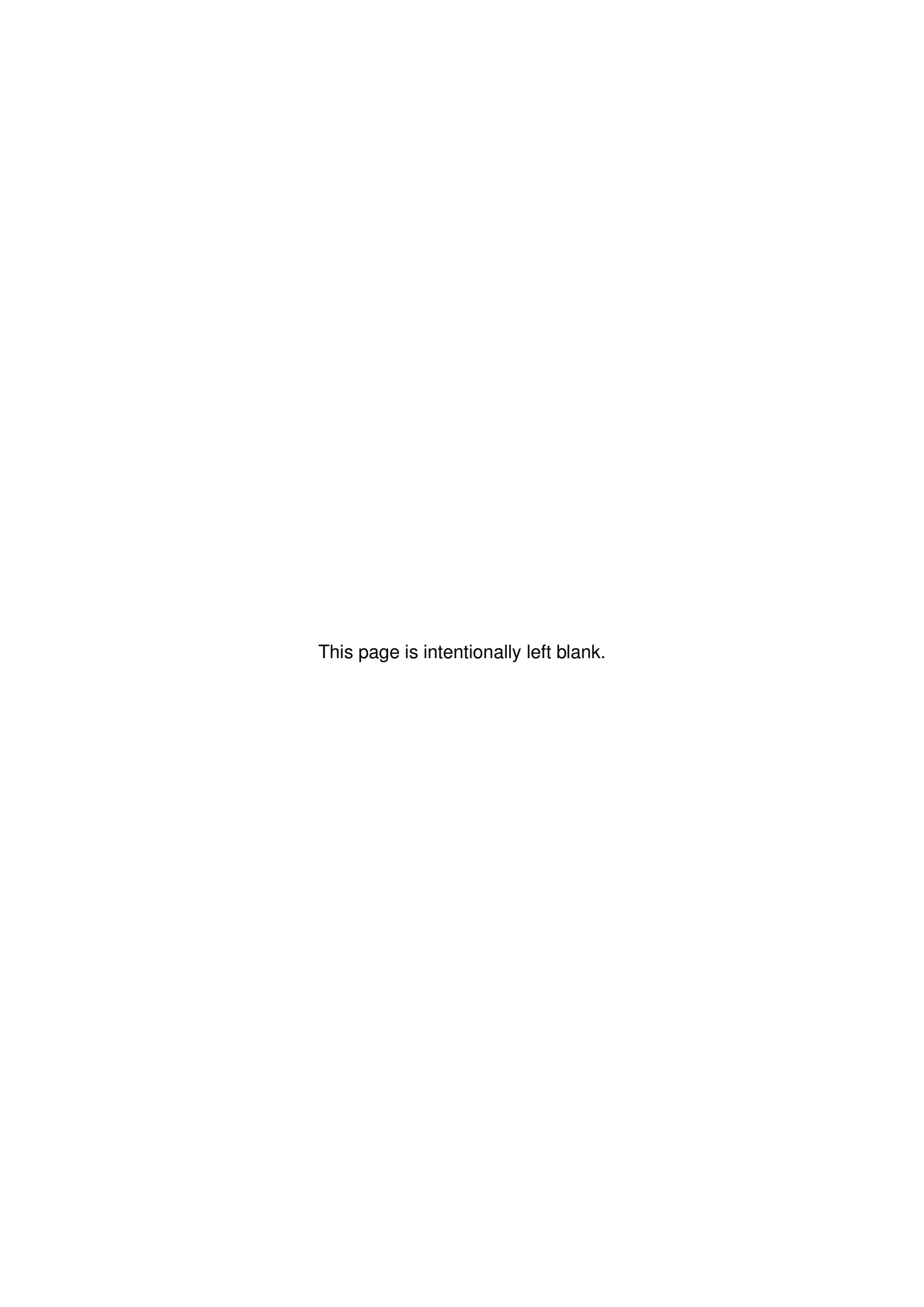
dr. Willem Huijbers(Philips Research) ir. Ad Denissen(Philips Research)

prof. dr. M. Huisman(Marieke) Formals Methods and Tools Group

dr. D. C. Mocanu(Decebal)
Data Management & Biometrics Group

Faculty of Electrical Engineering,
Mathematics and Computer Science
University of Twente
P.O. Box 217
7500 AE Enschede
The Netherlands





## **Acknowledgements**

This thesis marks the end of my 2-year journey at the University of Twente. It has been a time of great ups and downs, loss of motivation, and speed breakers on the way. However, during this time, I've grown a lot, personally and professionally, and I will always cherish this. During this journey, I got the chance to work with incredible people and have benefited a lot from their guidance and experience, and I would like to take this opportunity to express my sincere gratitude to those who helped me and contributed in different ways and aspects.

First of all, I would like to express my special gratitude to prof. dr. M. Poel(Mannes), for his unending support and encouragement during my years in Enschede. From connecting me to Philips Research to providing ample research opportunities, he has helped me a lot during this time.

I would also like to offer my sincere thanks to dr. Willem Huijbers and Ad Denissen, who are my supervisors from Philips Research. I have gained a lot of domain knowledge, ideas about neuroscience, and especially, how to think critically and inspect every aspect of a question from their expertise, and this would also go a long way to help me in my future career. I would also like to thank prof. dr. ir. D.C. Mocanu(Decebal), my university supervisor, for his extremely valuable insights during this long process. He has not only been a splendid guide, but also a motivating person, always guiding me to the correct path, even when things got harder. I would also like to thank prof. dr. Marieke Huisman for being on my thesis committee.

Next, I would like to thank my wonderful friends Sagnik, Rohan, and Arup, who has been with me since my school days and have been a constant support through thick and thin. Above all, I would like to thank my parents for their constant love and endless support, no matter what decisions I took for my life.

Anubrata Bhowmick Enschede, July 16, 2021

# **Contents**

Acknowledgements					
Αŀ	ostra	ct	viii		
Li	st of	acronyms	ix		
1	Intro	oduction	1		
	1.1	Motivation for research	2		
	1.2	Problem Formulation	3		
		1.2.1 Biomarkers from Statistical Analysis	4		
		1.2.2 Machine Learning based biomarkers	4		
	1.3	Research Questions	4		
	1.4	Research Contribution	5		
	1.5	Report organization	5		
2	Вас	kground & Related Work	6		
	2.1	Computational Neuroscience - History	6		
	2.2	Stress Neurobiology and Clinical Implications	7		
	2.3	Stress Resilience and Neuroimaging	8		
	2.4	Analysis of Neuroimaging Data	9		
	2.5	Deep Learning and Graph Neural Network	10		
		2.5.1 Deep Learning	10		
		2.5.2 Graph Neural Network	11		
3	Methodology 14				
	3.1	Data Acquisition	14		
	3.2	Data Preprocessing	15		
	3.3	Analysis & Stats. Inference Adjacency Matrices	18		
	3.4	Baseline Linear Modelling	19		
		3.4.1 Linear Regression	20		
		3.4.2 Logistic Regression	20		
		3.4.3 Support Vector Machine	20		

*Contents* v

D	Мар	ping of Region of Interest (ROI)s to Brain Regions	54
С	Visu	alization of biomarkers inside the brain	51
В	B.1	Importance of Normalization	<b>49</b> 49
Α	A.1	hine Learning Artificial Neural Network	<b>45</b> 45 47
Αŗ	pend	lices	
Re	eferen	ices	39
5	5.1	Clusion Limitations of study	<b>37</b> 37 38
	4.1	Experimental Settings  4.1.1 Preprocessing and Analysis  4.1.2 Baseline Modelling  4.1.3 Multi-layer Perceptron  4.1.4 BrainGNN  4.1.5 Feature Engineered Multi-layer Perceptron  Results  4.2.1 Preprocessing and Analysis	26 26 27 27 28 30 30 32 33 34 35
4		erimental Settings and Results	26
	3.7	Selection of Train-Validation-Test Data Split	23
	3.5 3.6	Multi-layer Perceptron	

# **List of Figures**

2.1 2.2	The stress system, Fig 1 [1]	8
3.1 3.2	Preprocessing pipeline [2]	15
3.3	and resilient mean matrix	18
3.4	to our adjacency matrix	22
3.5	have the accuracies recorded over the number of features Comparison the number of features over the best epoch count, signifying a linear trend in the training increase over increase in the features. On the x-axis, we have the number of features and on the	24
3.6	y-axis, we have the best epoch count	<ul><li>24</li><li>25</li></ul>
4.1	Co-registered subject-specific atlas over mean Functional Magnetic Resonance Imaging (fMRI) image shows that the newly created subject-	20
4.2	specific atlas is aligned perfectly over subject 5's mean fMRI image and hence, can be used for further preprocessing	30
	space, clearly indicating a normal distribution with a mean of little over 0	31

LIST OF FIGURES vii

4.3	Correlation map of subject 1 on the left hand side showing the same region values in the center and the upper and lower diagonal showing the left and right hemispheres of the brain, and distribution of correla-	
	tion values on the right side with a right tailed distribution	31
4.4	Connections of Resilience in matrix form from the 3 linear models, with Linear Regression in the left, Logistic Regression in the middle,	
	and Support Vector Machine on the right.	33
4.5	Training Accuracy and Loss for initial MLP model	33
4.6	MLP Model on various number of features. On the Y-axis, we have the	JU
4.0	accuracies of different models and on the X-axis, we have the number	
	of features.	34
4.7	Our MLP model on various number of iterations. On the y-axis, we have the train, test and validation accuracy values and on the x-axis,	0.
	we have the number of folds	34
4.8	BrainGNN Training/Validation Accuracy/Loss Plot	35
A.1	A classic example of Biological neuron	45
A.2	A classic example of Artificial neuron	45
A.3	Working of an artificial neural network	47
A.4	Bias Variance Tradeoff	48
C.1	Visualization of the biomarkers of stress resilience from Linear Re-	
	gression model	51
C.2	Visualization of the biomarkers of stress resilience from Logistic Re-	
	gression model	52
C.3	Visualization of the biomarkers of stress resilience from Support Vec-	
	tor Machine model	52
C.4	Visualization of the biomarkers of stress resilience from Multi-layer	
	Perceptron model	52
C.5	Visualization of the biomarkers of stress resilience from feature-engineer	
	Multi-laver Perceptron model	53

## **Abstract**

Developing psychopathology after a traumatic event has been a sought-after research for some time, and most of it has focused on the detrimental causes of anxiety, depression, or post-traumatic stress disorder. Earlier research showed a high degree of intra-individual variation in how individuals respond to stress. While no attempt has been made to understand resiliency using the available data, some researchers have tried to understand the same using a medical perspective.

In this thesis, we are developing methods to improve the estimation of functional brain connectivity using magnetic resonance imaging (MRI). This involves preprocessing and estimation of connectivity using state-of-the-art tools. It is then followed by the analysis of the correlation matrices, which is the baseline for understanding the significance of the connections.

The analysis is followed by research and development of various Machine Learning algorithms to understand whether complex mathematical algorithms can make sense of the data, and the correlations between them. This also led to another question as to whether they can perform better when there is not enough data for the analysis. This was followed by experimenting with state-of-the-art neural networks for brain analysis for a comparison of the brain regions and was concluded with the development of a new feature-engineered multi-layer perceptron framework that not only dealt with the low data problem but was also able to find robust biomarkers of brain resilience.

Our research resulted in finding biomarkers of brain resilience from various Machine Learning models, and showing that feature-engineered Multi-Layer Perceptron models can conclude better results as compared to data-hungry graph models, with the Feature Engineered Multi-Layer Perceptron (fe-MLP) model performing significantly better with around 64% classification accuracy as compared to 62% from the BrainGNN model. It also answers a significant question in research, pertaining to the fact that, if properly feature-engineered, multi-layer perceptron models can perform significantly better with less data, as compared to complex models.

# List of acronyms

**ANN** Artificial Neural Network

**fe-MLP** Feature Engineered Multi-Layer Perceptron

**fMRI** Functional Magnetic Resonance Imaging

ML Machine Learning

**MLP** Multi-Layer Perceptron

MNI Montreal Neurological Institute and Hospital

MRI Magnetic Resonance Imaging

**ROI** Region of Interest

**RSFC** Resting-State Functional Connectivity

**SVM** Support Vector Machine

## **Chapter 1**

## Introduction

Computational Neuroscience is a rapidly emerging field that enables us to better understand the brain's cognitive processes and information processing within the brain. By the time I finish writing this, a significant amount of activity has occurred inside my brain, which may be decoded through the study of neurons. The ultimate goal of computational neuroscience is to understand how electrical and chemical signals are used to represent and interpret information in the brain. It explains the biophysical mechanisms of computing in neurons, as well as computer simulations of neural circuits and learning models. This led to a lot of questions in the medical sector, as to how far can the experimentation in the brain be able to help clinicians provide personalized treatments and aid in solving various intra-personal issues.

Kietzmann et. al. [4] says that computational neuroscience seeks mechanical explanations for how the nervous system processes information to produce cognitive function and behavior. At the center of the field are its models, which are mathematical and computational representations of the system under investigation that link sensory stimuli to brain responses and/or neural responses to behavioral responses. These models range in complexity from simple to complicated. Artificial neural networks (ANNs), as described in Appendix A.1, have recently come to dominate various artificial intelligence (AI) disciplines. As the term "neural network" implies, these models are inspired by biological brains. Current Artificial Neural Network (ANN)s incorporate various characteristics of biological neural networks, enhancing computing efficiency and enabling them to do complex tasks ranging from perceptual (e.g., visual object and auditory voice identification) to cognitive (e.g., machine translation) to motor control (e.g., playing games or controlling a prosthetic arm). Apart from modelling complex intelligent behaviors, ANNs excel at predicting neural responses to novel sensory stimuli with a degree of precision that much exceeds that of any other model type now available.

Over the years, the biggest challenge has been the representation of brain signals in a form machines understand. One of the most important forms of translation was using functional magnetic resonance imaging (fMRI) images. Mathews and Jezzard [5] describe that functional magnetic resonance imaging (fMRI) with blood oxygenation level-dependent (BOLD) is a powerful technique for identifying brain activity in both healthy and ill humans. BOLD fMRI detects local changes in relative blood oxygenation, which are most likely the result of neurotransmitter action and so reflect local neural signaling. This has resulted in a data format that is easily represented in image form and can be used to perform modeling that, in turn, would be able to solve several computational neuroscience challenges.

#### 1.1 Motivation for research

This thesis work has been carried out in collaboration with Philips Research, in their brain, behavior, and cognition department, and the Leiden Medical Center. A new era of healthcare is dawning, one in which people increasingly take charge of their health and well-being, aided by an industry that is fast evolving and embracing technology in novel and ground-breaking ways, and Philips has always been at the forefront of breakthrough innovation. One of the goals of this department is to use these technologies to direct insights into our personality, mood, and physical functioning that can be used for context-sensitive health coaching. One of the leading research topics within Philips is Connected Care. In Connected Care, the focus is on investigating technologies and solutions that stimulate personal understanding of perception and mental issues. Amongst various such domains, one area where research is being carried out is stress resilience.

The sensation of being overwhelmed or unable to cope with mental or emotional pressure is referred to as stress. Stress is our body's reaction to pressure. Stress can be caused by a variety of conditions or occurrences in one's life. It is frequently triggered when we encounter something novel, unexpected, or threatening to our sense of self, or when we believe we have little control over a situation. Schneiderman et. al. [6] found that stressors have a significant impact on our mood, sense of well-being, behavior, and health. Acute stress responses in young, healthy people may be adaptive and do not usually hurt their health. However, if the threat is constant, especially in elderly or sick people, the long-term impact of stressors can be detrimental to health. The type, quantity, and duration of stressors, as well as an individual's biological sensitivity (i.e., genetics, constitutional factors), psychological resources, and learned coping methods, all affect the link between psychosocial stress and disease.

Hence, one of the main research areas of Philips is understanding stress resilience, and how it can be built up in an individual. Setroikromo et. al. [7] describes "stress resilience" as effectively coping with stressors and promptly returning to equilibrium, or "homeostasis," after the stress has passed. However, rather than stress resistance, I usually refer to effective coping as "stress optimization." Although recovering after the initial stress is an important aspect of stress management, the term resilience does not express the importance of active coping. Some individuals can easily cope with stress, while others develop psychiatric disorders, such as mood swings or anxiety after a traumatic event. Why some individuals are more resilient to stress is understudied, as most research is focused on the detrimental causes of anxiety, depression, or post-traumatic stress disorder. Therefore, in this project, we specifically searched for brain imaging biomarkers of stress resilience.

### 1.2 Problem Formulation

First responders, such as police officers, are more likely to experience traumatic events based on their work and a lower incidence of psychopathology has been reported in this population [8]. Such resilience is highly appreciated in this field of work, especially by first-line responders like the police and medical people. If anything, the current pandemic has shown the necessity of resilience in first-line responders in dire situations. Recruitment of first-line responders in the future could be heavily benefited by the prospect of resilience from fMRI imaging, as it can be used as a recruitment tool in the future, which can not only save the recruiting organization, but also the candidates who unknowingly take up jobs they might not be able to handle and have to give up on other opportunities. However, such a tool requires the explainability and understanding of the brain, especially the connections in the brain, called biomarkers. Our thesis aims to develop methods to improve the estimation of functional brain connectivity using functional magnetic resonance imaging (fMRI) [9]. Functional connectivity is measured by fMRI and the estimation of coherent activity across the brain. This includes the computation of coherence metrics, principal components, and separation of physiological noise. Functional connectivity gives us inherent information about the blood-oxidation level in the brain, which could show the inference of connections between two regions of interest. A common assumption is that the connectivities inside the brain have a significant difference between people who are resilient to stress, as compared to vulnerable people. We aim to do this in two different ways.

### 1.2.1 Biomarkers from Statistical Analysis

Our first task was to understand whether we could use the adjacency matrices, which are the matrices extracted after preprocessing the fMRI images and shows the correlation values between the ROIs of the brain, to rank the connections based on how important it is to understand resilience. We found the absolute mean group difference between the connections of resilient people and those who are vulnerable, resulting in a ranking of the connections that show the highest difference, effectively finding biomarkers of stress resilience.

### 1.2.2 Machine Learning based biomarkers

We replicated the ranking of the connections using linear methods to create a base-line method and used the state-of-the-art graph neural network to get a better classification score. However, we know that fMRI data is hard to get due to privacy issues and also the fact that people suffering from issues like psychopathology don't open up to doctors, and hence, it's a tough job to get enough data for research purposes. This brought up the issue of overfitting, as described in appendix A. We overcame the issue by creating a novel Machine Learning framework to replicate the biomarkers of stress resilience by effective feature-engineering with a multi-layer perceptron to get a good classification score with the robust ranking of the connections.

### 1.3 Research Questions

We define three major research questions that have been addressed in the thesis:

- Can we identify biomarkers of stress resilience using statistical methods from fMRI images?
- 2. Can we use Machine Learning algorithms to understand and explain biomarkers of stress resilience?
- 3. Can we overcome the problem of overfitting due to less data availability?
  - We came across a fundamental problem of overfitting (described in Appendix A.2) in Machine Learning while we were trying to find biomarkers using ML algorithms, which we had to overcome to find robust biomarkers of stress resilience.

### 1.4 Research Contribution

The overall goal of our thesis is to find biomarkers inside the brain that would aid clinicians in understanding resilience. The main contributions to our work are as follows:

- 1. We analyzed mean group differences between the resilient and vulnerable groups of people to check for connections that might be important for resilience.
- 2. We used different Machine Learning frameworks (Linear Regression, Logistic Regression, Support Vector Machine, and Multi-layer Perceptron) to draw upon rankings between the connections responsible for classification between the resilient and vulnerable groups of people, thereby finding biomarkers of stress resilience.
- 3. We used a state-of-the-art Graph Neural Network model, called BrainGNN [3] to analyze the connections of the brain, drawing upon the classification score to find the regions of interest that might strongly correlate with the classification score, thereby explaining which ROIs are more involved in stress resilience.
- 4. Both the standard Multi-Layer Perceptron (MLP) and BrainGNN encountered the problem of overfitting, which is a classic Machine Learning (ML) problem. To overcome that, we propose a new framework called feature-engineered Multi-layer Perceptron (fe-MLP) that uses linear model coefficients to reduce data dimensionality, and, in turn, be efficient at finding robust biomarkers of stress resilience.

## 1.5 Report organization

The rest of this thesis report is organized as follows. In chapter 2, we discuss previous advancements in the field of stress resilience and computational neuroscience leading up to my thesis work. Then, in chapter 3, we discuss the methodology that we used to carry out the research. We detail the experimental settings in chapter 4.1, followed by the results in chapter 4.2. Finally, in chapter 5, we conclude the final thesis with a summary of the work we carried out during the entire research process, and by outlining the limitations of our research along with the future steps that can be carried out to advance the research further.

## **Chapter 2**

## **Background & Related Work**

In this chapter, we will give a brief introduction to Computational Neuroscience, and how it has evolved over the years, from being a core clinical study to the computational aspects of it. We will also discuss the effects of Machine Learning on Computational Neuroscience, and how that is linked with stress resilience and our research.

## 2.1 Computational Neuroscience - History

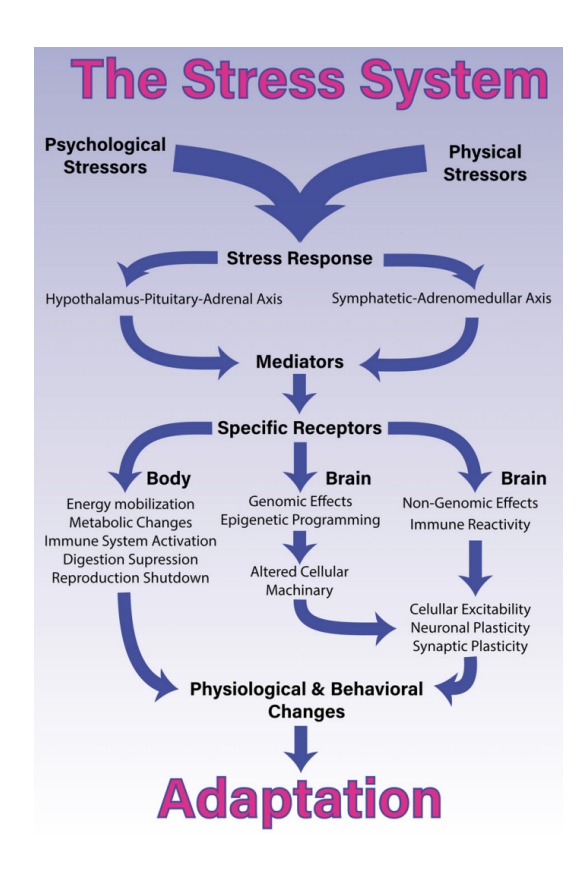
Neuroscience, alternatively referred to as Brain Science, is the study of the neural system's development, structure, and function. Neuroscientists study the brain and its relationship to behavior and cognition. Neuroscience, on the other hand, is concerned not only with the normal functioning of the nervous system but also with what happens to it when people suffer from neurological, psychiatric, or neurodevelopmental diseases. There are numerous branches of modern neuroscience, but the one we will focus on is Computational Neuroscience, which is concerned with understanding how brains compute by simulating and modeling brain functions using computers and by applying techniques from mathematics, physics, and other computational fields to study brain function [10].

According to Voss et al. [11], the term Computational Neuroscience was coined when a group of scientists intended to investigate the links between physical activity and exercise and the brain and cognition across the lifespan in healthy people. This resulted in an explosion of research in the field, ranging from cognition to physiological consequences to mental health difficulties, and the reality quickly sank in that the brain is an enormously complex organ with an abundance of research opportunities.

## 2.2 Stress Neurobiology and Clinical Implications

One of the most recent research that has captivated the neuroscience community comes from the study of neurobiology, specifically stress. According to Godoy et al. [1], stress is a key area of research in both basic and clinical neuroscience, owing to the pioneering historical studies undertaken by Walter Cannon and Hans Selye in the previous century, when the concept of stress emerged from a biological and adaptive perspective. Following that, further research was performed to further our understanding of stress, as illustrated in figure 2.1. Since then, it has been shown that the response to stressful stimuli is developed and triggered by the now-famous stress system, which integrates a diverse array of brain regions capable of detecting and interpreting events as real or potential risks. On the other hand, various types of stressors activate distinct brain networks, as illustrated in figure 2.2, necessitating fine-tuned functional neuroanatomical processing. This integration of information from the stressor may result in rapid activation of the Sympathetic-Adreno-Medullar (SAM) and Hypothalamic-Pituitary-Adrenal (HPA) axes, two critical components of the stress response. The stress response's intricacies extend beyond neuroanatomy and SAM and HPA axis mediators to the timing and duration of stressor exposure, as well as its short-and/or long-term consequences. The discovery of stress neuronal circuits and their interaction with mediator molecules across time is critical for understanding not just physiological stress reactions, but also their mental health repercussions. This expanded the scope of research into stress neurobiology because whenever there is a problem, there is usually an implicit quest for a solution. As a result, the study of stress resilience was initiated, and it has become a highly explored topic in recent years.

According to Baratta et al. [12], unfavorable events can affect the structure and function of the brain and are considered to be significant risk factors for depression, anxiety, and other mental diseases. However, because the majority of people who encounter undesirable or stressful life events do not suffer harmful consequences, it is critical to understand the mechanisms that promote resistance to the damaging effects of stress on a clinical level. Although considerable effort has been directed at the level of basic research toward discovering experimental settings that mitigate/amplify the impacts of an unfavorable experience, even when parameters are held constant, inter-subject variability in behavior exists. This has shifted the focus to elucidating how genetic and environmental factors interact to determine an organism's resistance to future adversity. The articles in this Research Topic summarize recent research targeted at deciphering the brain mechanisms underlying resilience and applying that knowledge to reduce susceptibility. This has resulted in numerous



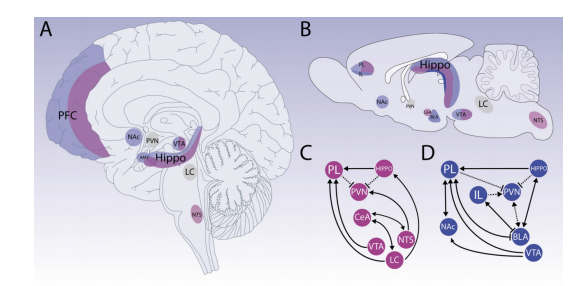


**Figure 2.2:** Neuroanatomy of stress, Fig 2 [1]

Figure 2.1: The stress system, Fig 1 [1]

clinical and technical studies on stress resilience, as well as a broad spectrum of implications across all fields of research.

## 2.3 Stress Resilience and Neuroimaging

A variety of disciplinary methodologies have been employed to elucidate the genetic, epigenetic, and brain circuit-level mechanisms underlying stress resistance. Wu et al. [13] present an in-depth overview of recent advancements in each of these analysis categories. Much of our understanding of the molecular mechanisms underlying human resilience has increasingly come from neuroimaging investigations. Werff et al. [14] compare the structural and functional changes associated with resilience in people who might have developed post-traumatic stress disorder (PTSD) in the aftermath of trauma. Due to the complexity of this construct, neuroimaging research on it is challenging. Werff et al. [15] described approaches for conceptualizing resilience. The few structural and functional neuroimaging studies designed to evaluate resilience have concentrated on alterations in brain regions involved in emotion and stress regulation networks.

Previous neuroimaging studies on resilience have compared resilience to psychopathol-

ogy following stress exposure, making specific resilience links difficult to make. Setroikromo et al.cite [7] used a three-group design with a non-trauma-exposed control group to distinguish resilience-related effects from psychopathology-related effects, and they examined resilience-specific cortical thickness and/or cortical surface area [16] correlates and their associations with psychometric assessments [17]. We measured the cortical thickness and surface area of the ROIs, as well as the entire brain. In ROI and whole-brain studies, there were no significant differences in cortical thickness or surface area between the resilient and control groups. The researchers discovered no correlation between resilience to extreme stress and measures of cortical thickness and surface area in a sample of Dutch police officers. Functional and structural connectivity methods [18], as well as innovative imaging task paradigms, are expected to improve neuroimaging of resilience in the future. This enabled us to delve deeply into the paradigm of image analysis to determine whether any specific connections or ROIs emerge that could be used to explain why some people are more resilient than others and be added as a supplement to the work already done by Setroikromo et al. [7].

## 2.4 Analysis of Neuroimaging Data

Resting-state functional connectivity reveals intrinsic, spontaneous networks that encapsulate the human brain's functional architecture [19]. To avoid potential confounding factors such as deceptive correlations based on non-neuronal sources, reliable statistical analysis used to discover such networks must incorporate noise sources. Gabrieli et al. [20] describe the functional connectivity toolbox Conn, which implements the component-based noise correction method [21] strategy for physiological and other noise source reduction, additional movement and temporal covariates [22] removal, temporal filtering, and windowing of the residual blood oxygen level-dependent (BOLD) contrast signal [23]. This toolbox is considered to be a state-of-the-art toolbox for neuroimaging data processing. It can be used to preprocess fMRI [24] pictures and generate adjacency matrices.

According to Aribisala et al. [25], displaying brain pictures in Montreal Neurological Institute and Hospital (MNI) space generates more noise than retaining them in real space. Real space represents the point-coordinate system in real-world photographs, whereas MNI representation compresses the images into a selected coordinate system, also referred to as standard space. We chose to conduct our analysis in real space, which required us to co-register [26] the images in real space with the mean fMRI images, to construct subject-specific atlases [27], which in turn aided us in creating adjacency matrices with real space representation. This enables us

to simplify our research techniques by establishing a common representation for subsequent analysis. Aribisala et al. [25] stated the purpose of this study was to compare the robustness of ROI analysis of magnetic resonance imaging (MRI) brain data in real space to that of MNI space analysis and to test the hypothesis that MNI space image analysis introduces more partial volume effect errors than does real space analysis of the same dataset.

## 2.5 Deep Learning and Graph Neural Network

The importance of machines in the field of Computational Neuroscience was realized with the rising amount of data, both textual and neuroimaging, and this led to several computer scientists using them to understand the underlying effectiveness of the connections.

### 2.5.1 Deep Learning

Filippi et. al. [28] stated that deep learning is a type of artificial intelligence that mimics the structure and organization of neurons in the brain as well as human intelligence. Deep learning has been used passionately in the field of medicine during the last decade, outperforming previously known methods. Deep learning algorithms, for example, have demonstrated their effectiveness in several fields of neuroscience, including the anatomical segmentation of specific brain areas, the delineation of brain lesions such as tumors, and the image-based prediction of various neurological illnesses. Deep learning is no longer simply an academic exercise, but a powerful tool in clinical practice, thanks to algorithm optimization, increased processing hardware, and access to a massive amount of imaging data.

According to Kietzmann et al. [4], computational neuroscience seeks mechanistic explanations for how the nervous system processes information to generate cognitive function and behavior. At the heart of the field are models, which are mathematical and computational representations of the system under investigation that connect sensory stimuli to brain responses and/or neural responses to behavioral responses. Deep neural networks (DNNs) have lately risen to prominence in a variety of fields of artificial intelligence (Al). As the term "neural network" implies, these models are inspired by biological brains. On the other hand, current DNNs neglect numerous elements of biological neural networks. These simplifications increase their computational efficiency, enabling them to perform complex feats of intelligence ranging from perceptual (e.g., visual object and auditory voice recognition) to cognitive (e.g., machine translation) to motor control (e.g. driving a car or controlling

a prosthetic arm). DNNs excel at accurately predicting neural responses to novel sensory stimuli, much above the accuracy of any other model type now known, in addition to their ability to describe complex intelligent behaviors. DNNs can have millions of parameters to capture the domain knowledge required for job execution success. Contrary to popular assumption, the computational characteristics of network units are determined by four easily manipulable factors: the input data, the network structure, the functional objective, and the learning algorithm. With complete access to the activity and connectivity of all units, advanced visualization techniques, and analytic tools for mapping network representations to neural data, DNNs provide a powerful framework for developing task-performing models and will generate significant insights in computational neuroscience.

### 2.5.2 Graph Neural Network

Graphs are a universal language for describing and analyzing items that have relationships or interactions. It is made up of nodes and the connections between them. Nodes frequently have attributes. Graphs are used to represent a wide range of data, from social media to neural networks. The primary issue with graphs is that they can be of any size and have a complex topological structure (i.e. no spatial locality). They do not have a set node ordering or reference point, and they are frequently dynamic with multimodal properties. The key idea for graph-based networks is to generate node embeddings [29] based on local network neighborhoods. Each network neighborhood defines a computation graph where information is aggregated from the neighbors using Neural Networks, which shows that each node is a summation of all the nodes with which it is connected over the total number of nodes (connected), and the addition of the surrounding node embeddings. The calculation to average the neighboring messages is as follows:

$$h_v^0 = x_v$$

$$h_v^{l+1} = \sigma(W_l \sum_{u \in N(v)} \frac{h_u^l}{|N(v)|} + B_l * h_v^l), \forall l \in \{0, ..., L-1\}$$

$$z_v = h_v^L$$

Here,  $W_l$  and  $B_l$  are the trainable weight matrices (i.e. what the machine learns from the data) and  $h_v^L$  is the final node embedding. These node embeddings are then sent to various Graph Neural Network layers to make a proper classification. The following are the most important network layers responsible for classification:

Batch Normalization: Stabilizes Neural Network Training.

- Re-center the node embeddings into zero mean.
- Re-scale the variance into unit variance.
- Dropout: Regularizes a Neural Network to prevent overfitting.
  - During training, with some probability p, we randomly set neurons to 0 (turn off).
  - During testing, they use all the neurons for computation.
- Attention/Gating: Controls the importance of a message, mainly through the application of activation functions.

The way Graph Neural Network handles unstructured graph data shows that these algorithms may be the optimal solution for our complicated problem. According to Zhou et. al. [30], many learning problems necessitate dealing with graph data that offers rich relationship information among elements. Graph neural networks (GNNs) are connectionist models [31] that reflect graph dependence through message passing between graph nodes. Graph neural networks, as opposed to ordinary neural networks, retain a state that can represent information from their neighborhood with arbitrary depth by aggregating the information from all their neighboring neurons, which is not the case for an ordinary neural network.

There are a few state-of-the-art graph-based models that are being researched continuously in the field of Computational Neuroscience. BrainNetCNN [32] is one of them. It is a convolutional neural network [33] framework for predicting clinical neurodevelopmental outcomes from brain networks. BrainNetCNN was used to predict cognitive and motor development outcome scores from preterm infants' structural brain networks. BrainNetCNN outperformed a fully connected neural network with the same number of model parameters on both localized and diffuse damage patterns. However, the BrainNetCNN is limited by the fact that it is only a classification algorithm and, hence, can not be used for our case, where we require more explainability and understand the features responsible for classification, which would allow us to understand the reasons for resilience. To overcome these shortcomings, we came across BrainGNN [3], an interpretable brain graph neural network for fMRI analysis. BrainGNN is a graph neural network (GNN) architecture for analyzing functional magnetic resonance imaging (fMRI) and identifying neurological biomarkers [34]. The fundamental goal of developing this framework was to improve transparency in medical image analysis, and BrainGNN includes ROI-selection pooling layers (Rpool) that emphasize prominent ROIs (nodes in the graph) for determining which ROIs are significant for prediction. Furthermore, on pooling results, regularization terms such as unit loss, topK pooling (TPK) loss, and group-level consistency (GLC) loss [35] were proposed to encourage proper ROI-selection and allow flexibility to maintain either individual or group-level patterns.

## **Chapter 3**

# Methodology

In this chapter, we will outline the methodology that helped us to find the biomarkers of stress resilience by statistical inference and with the help of machine learning. We start by outlining the Data Acquisition process in chapter 3.1, followed by Data Preprocessing in chapter 3.2 where the fMRI data is preprocessed to get the adjacency matrices. This was then followed by the analysis of the adjacency matrices and searching for initial biomarkers of stress resilience ranking using statistical inference in chapter 3.3. We then continued to find the same using Machine Learning methods in chapter 3.4 and chapter 3.5. We then used state-of-the-art BrainGNN to find the ROIs resilience, and check if this could outperform our methods. We concluded by developing a novel framework to avoid overfitting due to less availability, by measures of proper feature engineering, as described in section 3.7, and the framework in chapter 3.8.

## 3.1 Data Acquisition

We received the fMRI image dataset from the Leiden Medical Center. Resting-state functional Magnetic Resonance Imaging (MRI) scans were obtained from trauma-exposed executive personnel of the Dutch police force and non-trauma-exposed recruits from the police academy. Participants were divided into three groups: a resilient group (n = 19; trauma exposure; no psychopathology), a vulnerable group (n = 18; trauma exposure, psychopathology) and a control group (n = 9; no trauma exposure, no psychopathology) as shown in table 3.1. Resting-State Functional Connectivity (RSFC) of the three networks of interest were compared between these groups, using independent component analysis and a dual regression approach.

Group	No. of participants
Resilient	19
Vulnerable	18
Control	9

Table 3.1: fMRI resilience dataset from Leiden Medical Center

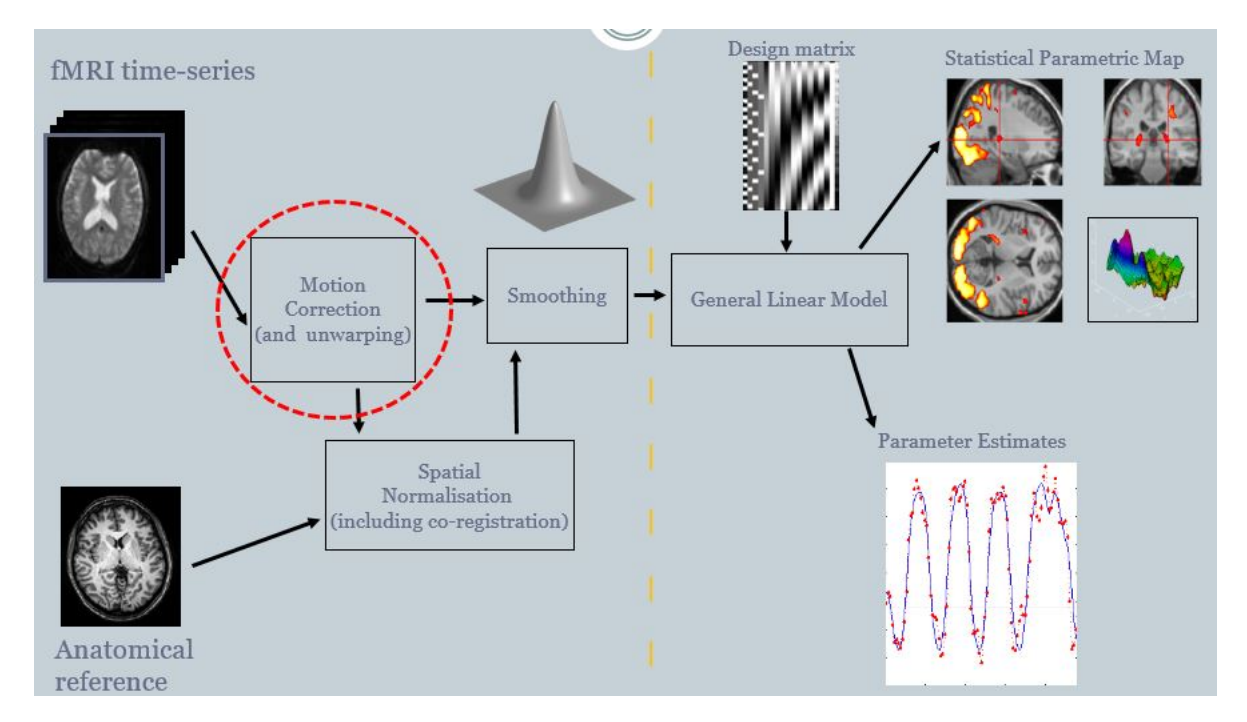


Figure 3.1: Preprocessing pipeline [2]

### 3.2 Data Preprocessing

Initially, the anatomical images received were divided into 91 neocortical regions of interest per the Hamburg nonMNI atlas, provided by the Hamburg team of Philips Research. We started by binarizing the brain regions into 62 neocortical regions per the Desikan atlas [36], by creating subject-specific atlases for each subject in native space. Another instance of the same was created in MNI space to understand which representation of the data stores more information and less noise.

Signals in crude fMRI information are impacted by numerous components other than mind action, like breath, head development, and so forth. These may prompt an expansion of the remaining change and decrease affectability. To tackle these issues, we need to preprocess the information appropriately. We chose to utilize the utilitarian tool CONN [20] for this. We began preprocessing by performing subject movement assessment and remedying by realigning and unwarping the information. Realigning realigns the pictures procured from similar subjects after some time

and matches them spatially. Realignment can be separated into the accompanying advances:

- Registration: Assesses 6 parameters for differences between the source pictures and the reference image (1st picture in the series).
- <u>Transformation</u>: Here, each picture is coordinated with the main picture of the time series, dependent on the changing boundaries of the first cut.
- Interpolation: B-Spline interpolation [37] is carried out.

Even after realignment, there is still a great deal of difference, which may prompt loss of affectability or particularity. We continued to unwarp the information to eliminate some undesirable changes without eliminating "valid" actuations.

As clarified in [38], cuts can't be obtained at the same time because of the idea of the fMRI procurement conventions, and, accordingly, may be briefly skewed from one another. Thus, we continued with the Slice-Time Correction step in the pipeline, the impacts of which are referenced in [39].

Potential anomaly examines are recognized from the noticed worldwide BOLD sign and the measure of subject movement in the scanner in the subsequent stage. Acquisitions with outline astute relocation above 0.9mm or worldwide BOLD sign changes over 5 standard deviations are hailed as likely anomalies. Casing insightful uprooting is processed at each time-point by considering a 140x180x115mm bounding box around the mind and assessing the biggest dislodging among six control focuses set at the focal point of this jumping box. The worldwide BOLD sign change is processed at each time point as the adjustment of the normal BOLD sign inside SPM's worldwide mean veil scaled to standard deviation units.

The following stage is co-registration [26] of pictures. The primary capacity of this progression is to accomplish coordination between methodology and intra-subject information. The realigned utilitarian information should be connected to the primary information. The underlying information has anatomical localization, and the practice has a BOLD sign. We need these two to cover, which prepares for improved interpretation into MNI/local space. This is trailed by spatial standardization, which is a type of co-enlistment between subjects. The principal capacity of this progression is to twist pictures of people into a similar standard space. The significance of standardization has been written down in B.1.

Useful and anatomical information is standardized into standard MNI space and divided into grey matter, white matter, and CSF tissue classes utilizing the SPM12 bound together division and standardization method as expressed in [40]. This strategy iteratively performs tissue arrangement, assessing the back tissue likelihood

maps (TPMs) from the force upsides of the reference utilitarian/anatomical picture, and enlistment, assessing the non-straight spatial change best approximating the back and earlier TPMs, until intermingling. Direct standardization brought together division and standardization techniques independently of the practical information, utilizing the mean BOLD sign as a reference picture, and of the underlying information, utilizing the crude T1-weighted volume as a reference picture. Both utilitarian and anatomical information are re-inspected to a default 180x216x180mm bouncing box, with 2mm isotropic voxels for useful information and 1mm for anatomical information, utilizing fourth request spline addition.

Following the preprocessing pipeline, a couple of yield NIfTI <sup>1</sup> documents are worked out, comprising of the meaning of the fMRI pictures and some others. We then, at that point, utilize our recently made subject-explicit chart books and co-register them over the fMRI preprocessed information before moving them on to the denoising pipeline. Co-enlistment over mean fMRI information for more than one subject can be found in Figure 4.1.

The next stage is passing the data through the CONN denoising pipeline. CONN's denoising pipeline<sup>2</sup> combines two general steps: linear regression of potential confounding effects in the BOLD signal, and temporal band-pass filtering.

Denoising has the effect of reducing the impact of artifactual variables on useful availability estimates. This effect can be best illustrated by examining the conveyance of useful network esteems between haphazardly chosen sets of focuses inside the cerebrum when denoising. Considering the BOLD sign after a standard insignificant preprocessing pipeline (before denoising), FC conveyances show very enormous between-meeting and between-subject inconstancy, and slanted circulations with differing levels of positive inclinations, steady with the impact of worldwide or huge scope physiological and subject-movement impacts. Following denoising, FC circulations exhibit broadly concentrated dispersions, with hardly discernible larger tails on the positive side, and significantly decreased inconstancy between meetings and between subjects.

The last stage in the preprocessing pipeline is to compose connectivity (correlation) frameworks utilizing the Seed-Based Connectivity measures<sup>3</sup>. Seed-based availability measurements portray the network designs with a pre-characterized seed or

<sup>&</sup>lt;sup>1</sup>https://radiopaedia.org/articles/nifti-record format

<sup>&</sup>lt;sup>2</sup>https://web.conn-toolbox.org/fmri-methods/denoising-pipeline

<sup>&</sup>lt;sup>3</sup>https://web.conn-toolbox.org/fmri-techniques/network measures/seed-based

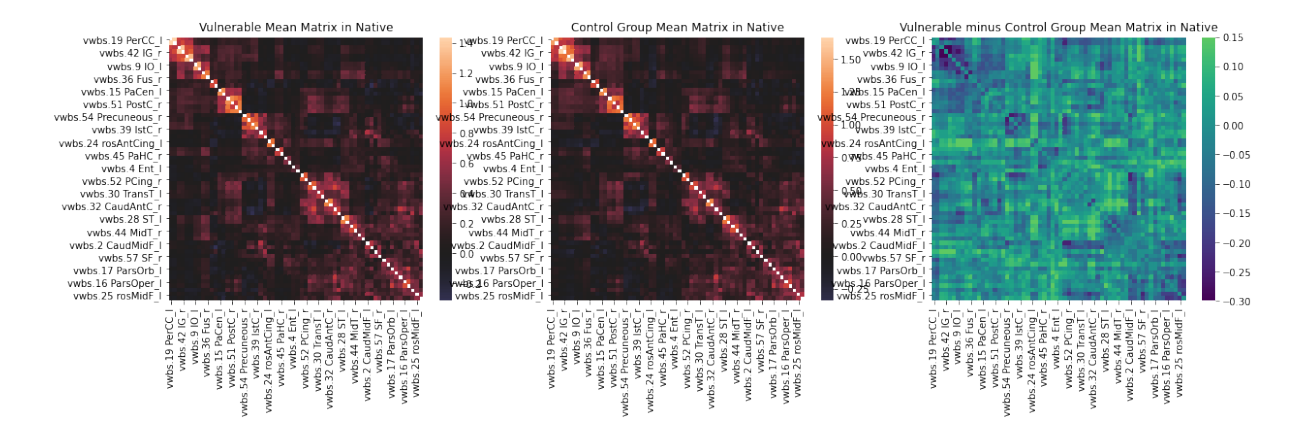


**Figure 3.2:** The graph on the left represents the vulnerable mean matrix, the graph in the middle represents the resilient mean matrix, and the graph on the right represents the difference between the vulnerable and resilient mean matrix.

ROI (Regions of Interest). This technique utilizes Seed-Based Connectivity maps utilizing the Fischer-changed<sup>4</sup> bivariate relationship coefficients between an ROI BOLD time-arrangement and every individual voxel time-arrangement:

$$r(x) = \frac{\int S(x,t)R(t)dt}{(\int R^2(t)dt \int S^2(x,t)dt)^{0.5}}$$
$$Z(x) = tanh^{-1}(r(x))$$

However, after the completion of the entire preprocessing pipeline, we concluded that 1 subject was completely out of sync and failed to preprocess properly. Hence, we decided to ignore that subject and the output from the final stage are adjacency matrices of the 45 subjects with dimensions of 62x62, comprising of all the ROIs of the brain.

## 3.3 Analysis & Stats. Inference Adjacency Matrices

Our initial analysis started by looking at the adjacency matrices from the preprocessed fMRI images. The combined distribution of all the subjects was observed, which resulted in Figure 4.2. We also checked the distribution of individual subjects and understood whether any subjects/groups showed similar distributions in comparison to others, and the result is shown in Figure 4.3.

On initial analysis of the adjacency matrices, no connections popped out due to the overall adjacency matrices being sparse, and hence, important connections were all

<sup>&</sup>lt;sup>4</sup>https://blogs.sas.com/content/iml/2017/09/20/fishers-transformation-correlation.html

over the matrix. That's why a clustering mechanism was devised by Chen et. al. [41] which states that for pattern recognition, a dendrogram that visualizes a clustering hierarchy is frequently combined with a reorderable matrix to effectively cluster the important connections together and find the activations within the adjacency matrices. This resulted in reordered adjacency matrices as shown in figure 3.2.

One way of understanding which connections might be responsible for stress resilience was to understand the difference between the connections in the resilient and vulnerable groups. We took the difference between the mean matrices of all the subjects of the resilient and vulnerable groups as shown in figure 3.2. Luthar et. al. [42] states that the higher the difference between the connections of both groups, the more important those connections are in explaining resilience. We took the absolute value of the difference in the connections and ranked them in descending order. The resulting biomarkers are shown in table 4.3.

## 3.4 Baseline Linear Modelling

We developed baseline linear models to understand the connections responsible for resilience. A baseline model is always the first step to understanding whether the machine learning models can make sense of the dataset. We decided to do a comparison of the linear models to find the baseline connections. We decided to use the entire dataset for baseline modeling. However, the number of connections (features) is way too high for interpretation. Therefore, we decided to remove the duplicate connections (connections from one hemisphere of the brain) from the adjacency matrices. We removed the healthy control subjects from the dataset, leading to a smaller dataset. The columns comprising of participant\_id, sex, and age have also been removed as they played no part in improving the predictability of the Machine Learning models. The adjacency matrices have been flattened to be used as features for linear models. We also converted the categorical column of the diagnosis (the value we have to predict) column of the dataset to numerical to be made interpretable by the linear models. The correlation values that resulted from the preprocessing pipelines are the values to be used for features, and these represent the correlation values between the connections between the regions of the brain. We split the dataset into 70% training data and 30% testing data. We decided to run the model k-times for interpretability.

We then checked for the average accuracy over k iterations of the Logistic and Support Vector Machine (SVM) models and found biomarkers of brain resilience.

### 3.4.1 Linear Regression

We began with a Linear Regression model and chose to fit the complete data set. All of the obtained connections were utilized to fit the model with coefficients w = (w1,..., wp) to minimize the residual sum of squares between observed targets in the dataset and anticipated targets using the linear approximation. We used Ordinary Least Squares (scipy.linalg.lstsq) wrapped as a predictor object to fit the data and predict the coefficients of determination  $(R^2)$ .

We then used the absolute values of the model coefficients from the Linear Regression model to rank the features responsible for the coefficients of determination  $(R^2)$ . We sorted the features based on their importance, and repeated the same for over k-folds, resulting in an order-independent ranking of the features of importance.

### 3.4.2 Logistic Regression

We followed the Linear Regression Model with a separate Logistic Regression model. The training algorithm uses "cross-entropy" loss, with L2 regularization, and a one-vs-rest (OvR) scheme and is trained on the entire dataset for 100 iterations. We have also used L-BFGS-B – Software for Large-scale Bound-constrained Optimization solver<sup>5</sup>, which supports L2 regularization.

We selected the model coefficients from the models which predicted better than chance (over 50% accuracy) over k-folds to rank the features responsible for prediction. We sorted the features based on their importance, and repeated the same for over k-folds, resulting in an order-independent ranking of the features of importance.

### 3.4.3 Support Vector Machine

Following that, the Support Vector Machine model was used to complete the linear set. This implementation is based on the libsvm<sup>6</sup> Support Vector Machine (SVM) package. We used Grid Search to identify the optimal Support Vector Machine settings, which is a suggested strategy because the right choice of the regularization parameter (C) and kernel coefficient (gamma) is important to the Support Vector Machine (SVM)'s performance and should be exponentially spaced apart to get good values. The parameter C, which is shared by all SVM kernels, trades off the misclassification of training samples against the decision surface's simplicity. Gamma quantifies the influence of a single training example.

<sup>&</sup>lt;sup>5</sup>http://users.iems.northwestern.edu/ nocedal/lbfgsb.html

<sup>&</sup>lt;sup>6</sup>https://www.csie.ntu.edu.tw/ cjlin/papers/libsvm.pdf

These parameters were utilized to generate classification scores, in which we used the model coefficients from models that predicted better than chance (more than 50% accuracy) over k-folds to rank the predictive characteristics. We sorted the features by relevance and repeated the process over k-folds, resulting in an order-independent ranking of the most significant features.

## 3.5 Multi-layer Perceptron

After the creation of baseline linear models, we decided to find the features responsible for resilience using a multi-layer perceptron. A perceptron is a computer model or computerized system that is designed to mimic or simulate the brain's ability to perceive and differentiate. We know that the small dataset might be a factor during our experiments. So, we decided to run the model for 'k' number of times, where 'k' is chosen as a random number that fits the dataset well, to remove the factor of overfitting, as was explained by running the model initially. We divided the dataset into 49-21-30 splits, as described in chapter 3.8. We split the dataset k-times with various subjects being in the various datasets (train-validation-test) for different folds, hereby removing the overfitting factor. For each fold, we sample the features 100 times to make the features order-independent.

The Multi-layer perceptron model consists of 4 Dense layers [43] and 4 Dropout layers [44] with Rectified Linear Unit (ReLU) activation function [45], and a 'sigmoid' activation function [46] in the last layer to get the probability values for both the classes after classification. We have also used Adam Optimizer [47] and Sparse Categorical Cross Entropy as the loss function. The model converged fast and overfitted tremendously after 50 epochs. So, we decided to train the model for a max of 50 epochs and employed early stopping, where we selected the model with the highest validation accuracy.

This model was then tested for classification on the test set and the features were then separated and checked over k-folds to see which features were responsible for most of the predictions. This allowed me to create a top-30 list of the most important features (connections) responsible for resilience.

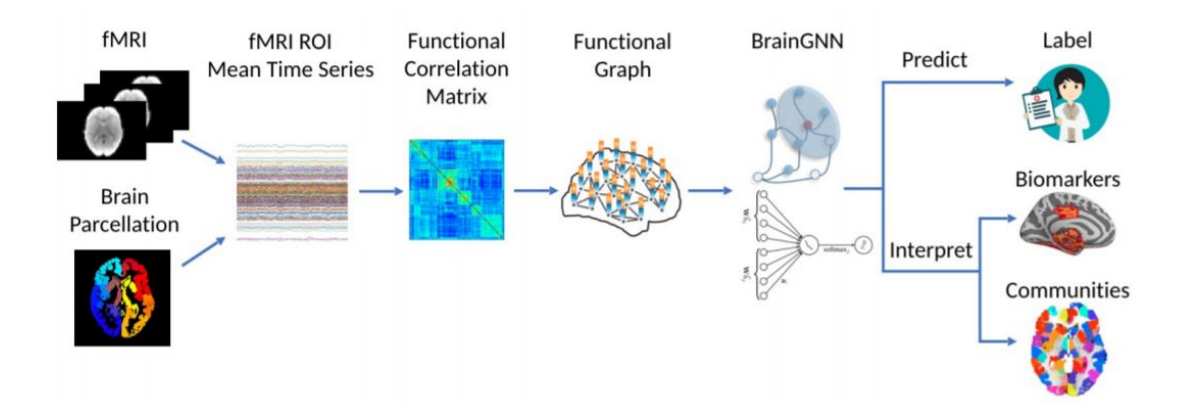


**Figure 3.3:** BrainGNN [3]: Interpretable Graph Neural Network for Brain Graph Analysis. The functional correlation matrix in this image is equivalent to our adjacency matrix.

## 3.6 Graph Neural Networks

Our research included exploring a different form of Machine Learning model that could handle graph-based data. As our adjacency matrices are in the form of graphs, we explored various graph-based Machine Learning models that could handle this data. This is how we came across the state-of-the-art Graph Neural Network method, BrainGNN [3]. We decided to implement the state-of-the-art Brain Graph Neural Network from the paper by Li et. al. [3], which consists of the Pooling Regularized Graph Neural Networks [48], where the terms Pooling and Regularized Graph are termed in each layer of the neural network, followed by a classification layer, which can be seen in Figure 3.3.

We started by creating a graph dataset from the adjacency matrices that received post-processing from the fMRI images, as described in chapter 3.2. Graph neural networks are usually trained in batches. However, due to the small dataset, we decided to encapsulate the entire dataset in a single batch. The adjacency matrices were converted into graphs using the networkx library and self-loops were removed. The edge indexes and attributes were stored separately, along with the number of nodes.

As PyTorch is our main framework for the Graph Neural Network model, the edge attributes were stored in a list and then converted into tensors for further processing. Similarly, the label list, adjacency matrices, and the edge indexes were converted into PyTorch tensors. Then the entire lists were encapsulated in a Data format, and then divided into 49-21-30(train, validation, and test) split for training purposes. The train, test, and validation splits were then converted into PyTorch Data format from

the Dataloader<sup>7</sup> and sent to training.

There are two proposed models for Pooling Regularized Graph Neural Networks, namely LI\_NET [49] and NNGAT [48]. We decided to proceed with LI\_NET for our analysis since LI\_NET handles high data dimensionality better than the NNGAT layer. The next option we had was to choose which pooling layer would better suit our research. We chose the TopKPooling [35] [50] [51] layer, which is mainly used for data reduction and interpreting biomarkers. The last layer is a simple classification layer, using the softmax function, to provide the probability of the respective classes. The results of the training are mentioned in Section 4.2.5.

## 3.7 Selection of Train-Validation-Test Data Split

Before proceeding with the Feature Engineered Multi-layer Perceptron, we decided to find the proper train-validation-test split that can be optimally used for preventing overfitting. We used a plethora of train-validation-test splits for various Multi-layer Perceptron models over various epochs, to see which split performed the best in terms of train-test-validation accuracy. Apart from the train-validation-test split, this model also helped us to understand the best epoch for any number of features assigned, ultimately converging on the best number of features responsible for resilience. The results are mentioned in chapter 4.2.6.

## 3.8 Feature Engineered Multi-layer Perceptron

Due to the rampant overfitting of the multi-layer perceptron and the Graph Neural Network, we decided to employ a different framework that would prevent overfitting. This led to me creating a Feature Engineered Multi-layer Perceptron, which uses model coefficients from a logistic regression model, which can be used to rank the top k-features, as described in chapter 3.4.2. We then selected the top 30 features (connections) and separated them into the splits resulting from chapter 3.7. These features are then sent to the multi-layer perceptron as described in chapter 3.5 and then the top 30 connections, ranked by the Logistic Regression models, are made order-independent by removing overfitting due to the aforementioned feature engineering. This then allows us to select the top-k features responsible for resilience. The results from this model can be seen in section 4.2.6.

Based on the folds decided in chapter 4.1.5, we checked the training and validation

<sup>&</sup>lt;sup>7</sup>https://pytorch.org/docs/stable/data.html

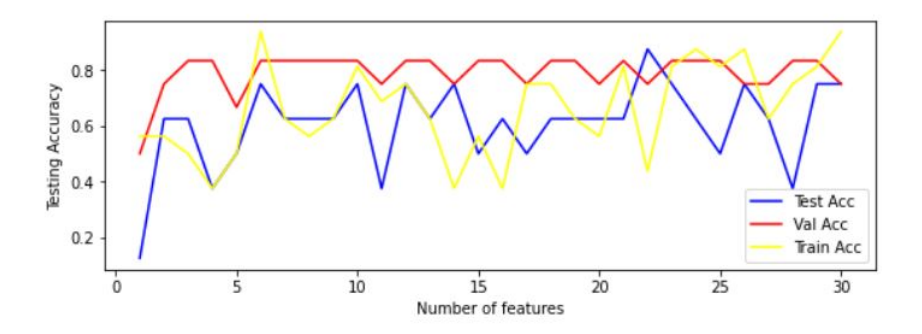


**Figure 3.4:** Training, Validation and Testing Accuracy for dataset with 70-30 split. On the x-axis, we have the number of features and on the y-axis, we have the accuracies recorded over the number of features.

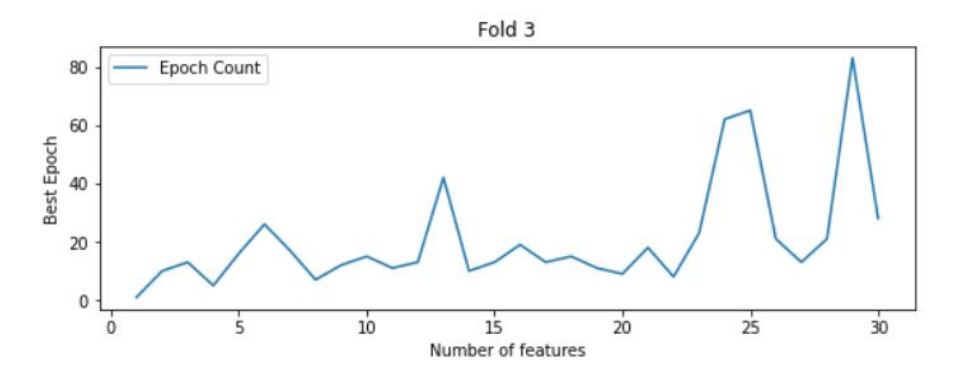
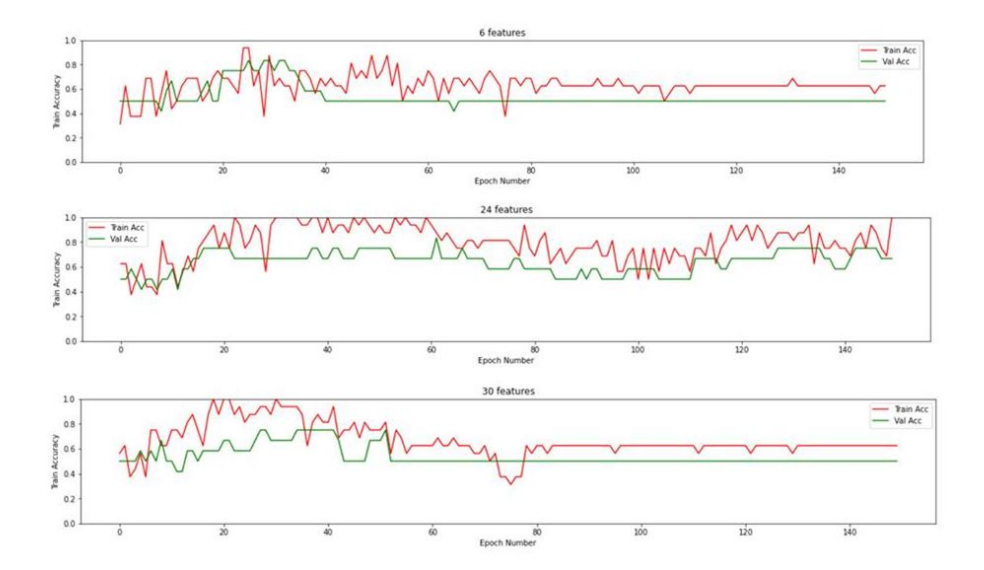


Figure 3.5: Comparison the number of features over the best epoch count, signifying a linear trend in the training increase over increase in the features. On the x-axis, we have the number of features and on the y-axis, we have the best epoch count.

accuracy of different folds and how erratic they are. Fold 3 having a 70-30 dataset split has performed the best, with the accuracies being less erratic as compared to the other folds, as seen in Figure 3.4. Also, a comparison between the features and epochs was analyzed to see if there is a linear trend between them, as seen in figure 3.5.

The training and validation accuracies were observed over the epochs, which can be seen in the figure 3.6 and we have concluded that the top 10, 24, and 30 features represent the lowest training and validation errors, while having 75%, 62.5%, and 75% testing classifications respectively.

This gave us conclusive evidence of the perfect fit for the dataset, even though we don't have enough data to run complicated Deep Learning models. So, we decided on the **final split** of **49%-21%-30%** to run all our Linear and MLP models on, and found out that **10 features** perform the best classification score. We also determined



**Figure 3.6:** Training vs Validation curve over epochs. On the x-axis we have the number of epochs and on the y-axis, we have the train/validation accuracy.

that we don't need more than **50 epochs** for the MLP models and fe-MLP models.

## **Chapter 4**

# **Experimental Settings and Results**

## 4.1 Experimental Settings

### 4.1.1 Preprocessing and Analysis

We used the CONN Toolbox<sup>1</sup> to preprocess our fMRI dataset. This required coregistration of anatomical images in native space. Hence, we had to binarize the ROIs of the brain from 1-62, stating the images comprise 62 regions, and any region more than 62 had to be made 0.

### 4.1.2 Baseline Modelling

#### **Hyper-parameter Optimization**

We have employed several hyperparameters for the 3 different linear models.

For the linear regression, we have used fit\_intercept as True, normalize as False, positive as False.

For the logistic regression model, we have used penalty as I2, tolerance for stopping criteria(tol) as 0.0001, C as 1.0, fit\_intercept as True, random\_state as None, solver as lbfgs, max\_iter as 100, multi\_class as auto, and verbose as 0.

For the SVM model, we have used C as 10, kernel as linear, degree as 3, gamma as 0.001, coef0 as 0.0, shrinking as True, probability as False, tol as 0.001, cache\_size as 200, class\_weight as None, verbose as False, max\_iter as -1, decision\_function\_shape as ovr, break\_ties as False, and random\_state as None.

<sup>&</sup>lt;sup>1</sup>https://web.conn-toolbox.org/

### 4.1.3 Multi-layer Perceptron

#### **Hyperparameter Optimization**

For the MLP model, we have used **Adam Optimizer** with a starting **learning rate** of **0.1**, **Sparse Categorical Cross Entropy loss function**, **4 dense layers** comprising of **1891**, **512**, **256**, and **64** neurons respectively, with **Rectified Linear Unit activation function**, along with **4 dropout layers** with **0.4 probability**. The final Dense layer comprises of **2 neurons** and **sigmoid activation function** in order to get the probability of the two classes for classification.

#### 4.1.4 BrainGNN

#### **Training and Testing**

We started by converting the adjacency matrices into brain graphs, by reading the individual MatLab files of each subject. We started by selecting the first 62 columns from the MatLab files, which are the connections between the ROIs of the brain, and converting the NaN values to 0. We then removed the self-loops and created edge index and edge attribute lists for all the subjects. For each subject, we have a list of all the edge attributes (correlation values), edge index (the connections), and adjacency matrices. This was converted into a Data format<sup>2</sup>.

#### **Hyperparameter Optimization**

We tuned the hyper-parameters in accordance to the needs of our research. We kept the **number of epochs** to **100** as the data seemed to overfit tremendously after that. The **batch size** has been determined to fit the entire dataset together well, so we kept it at **36**, representing the entire dataset. The **learning rate** was kept at **0.001** and **Adam Optimizer** has been used with a **weight decay factor** of **1e-2**. A **regularization factor** of **0.2** has been used for **L2 regularization**. We have kept **1000 GNN layers** in order to avoid overfitting. We used **BCE loss** for the **distance loss measurement**, the **pooling method** we used was **TopkPooling**, and the **model** we used was **NNGAT**.

<sup>&</sup>lt;sup>2</sup>https://pytorch.org/docs/stable/data.html

Model	Training Accuracy	Testing Accuracy
Logistic Regression	-	58%
Support Vector Machine	-	60%
Multi-layer Perceptron	57.3%	61.8%
BrainGNN	72%	62%
feature-engineered Multi-layer Perceptron	72%	64%

Table 4.1: Overview of all the models

#### 4.1.5 Feature Engineered Multi-layer Perceptron

#### Finding the perfect fit

To find the most reliable biomarkers, we used the model coefficients from the Logistic model to rank the features, followed by sending the features incrementally to a multi-layer perceptron. The dataset was split into 4 different folds (90%-10%, 80%-20%, 70%-30%, and 60%-40%) to avoid overfitting. For each fold, we checked the training and validation accuracy to show how erratic they are when increasing the number of features over epochs.

For the multi-layer perceptron, we have performed hyperparameter tuning to optimize the model, as mentioned in chapter 4.1.3. We ran the model for a maximum of 100 epochs, as most of the features converged way before the 100 mark. Early stopping has been employed to save the best model (model having the highest validation accuracy), which has then been used for the test dataset.

### 4.2 Results

During the research, we came across various results that drove me towards my final goal of finding biomarkers of brain resilience, which have been described below. In chapter 4.2.1, we find the results of the preprocessing pipeline, i.e. the adjacency matrices. We then discuss the results from our baseline linear models in section 4.2.3, followed by the results from the BrainGNN in section 4.2.5 and we end with the results from the feature engineered Multi-layer perceptron in chapter 4.2.6.

The overview of all the modeling has been tabulated in 4.1, and the biomarkers of brain resilience can be seen in table 4.2. Another important aspect of these rankings can be seen visually in Appendix C.

LinReg-	Score	Score LogReg-	Score	Score SVM-Rank	Score	Score MLP-Rank	fe-MLP-	Score	Score BrainGNN-
Rank		Rank					Rank		Rank
PerCC_r -	0.11	PerCC_r -	0.27	ParsOper_I -	0.03	PerCC_r -	PerCC_r -	0.31	PerCC_r
ST_r		ST_r		ST_I		ST_r	ST_r		
RosMidF_I -	0.11	ParsOper_I -	0.19	PerCC_r -	0.03	ParsOper_I -	ParsOper_I -	0.29	ParsOper_r
ParsOper_r		RosMidF_r		ST_r		ST_	ST		
CaudAntC_r -	0.10	RosMidF_I -	0.18	RosMidF_I -	0.03	RosMidF_I -	RosMidF_I -	0.29	SF_r
SF_r		ParsOper_r		ParsOper_r		ParsOper_r	ParsOper_r		
PCing_r -	0.10	CaudAntC_r -	0.18	CaudAntC_r -	0.02	CaudAntC_r -	CaudAntC_r -	0.28	PCing_r
SF_r		SF_r		SF_r		SF_r	SF_r		
ParsOper_l -	0.10	PerCC_I -	0.17	Ist_I - Ros-	0.02	ParsOper_r -	ParsOper_I -	0.25	RosMidF_r
RosMidF_r		ST_r		MidF_I		RosMidF_I	RosMidF_r		
PerCC_I -	60.0	PCing_r -	0.10	ParsOper_I -	0.02	lstC_I - Ros-	IstC_I - Ros-	0.25	ST_r
ST_r		SF_r		RosMidF_r		MidF_I	MidF_I		
CaudMidF_I -	60.0	SF_I - PC-	60.0	PCing_r -	0.02	Fus_r - Pars-	Fus_r - Pars-	0.21	CaudMidF_I
PCing_r		ing_r		SF_r		Triang_r	Triang_r		
RosMidF_I -	60.0	SF_I - SM_r	0.03	PerCC_I -	0.01	PCing_I - SF_I	PCing_r -	0.21	SM_r
SM_r				ST_r			SF_r		
SF_I - PC-	90.0	CaudMidF_I -	0.03	Fus_r - Pars-	0.01	PerCC_I -	PerCC_I -	0.19	SF_I
ing_r		PCing_r		Triang_r		ST_r	ST_r		
RosMidF_l -	90.0	ParsOper_l -	0.01	- l <u>T</u> II	0.01	PerCC_I -	PerCC	0.17	RosMidF_I
ParsTriang_r		SM₋r		RosAntC-		PerCC_r			
				ing_r					

Logistic Regression, Support Vector Machine, Multi-layer perceptron, to feature-engineered Multi-layer perceptron and Table 4.2: All biomarkers ranked in accordance to the Machine Learning models and their scores in order, from Linear Regression, BrainGNN. The connections/regions of interest is described in appendix ??

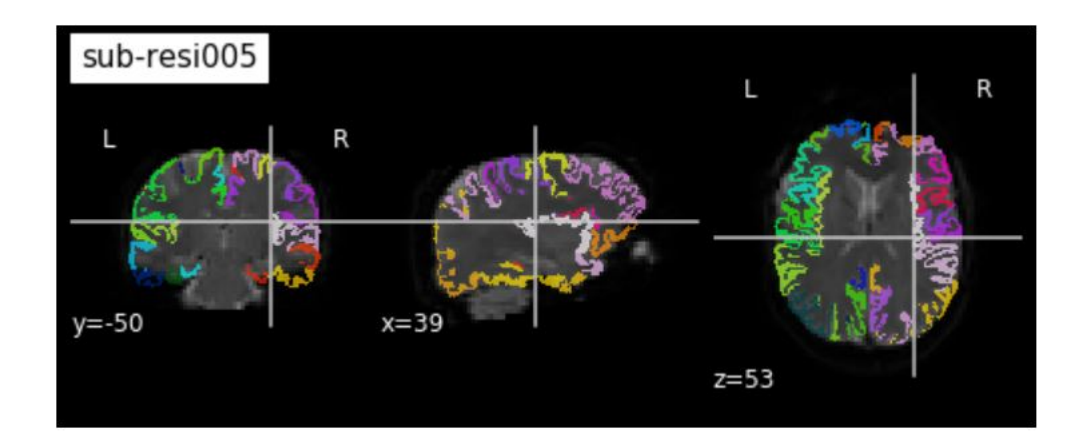


**Figure 4.1:** Co-registered subject-specific atlas over mean fMRI image shows that the newly created subject-specific atlas is aligned perfectly over subject 5's mean fMRI image and hence, can be used for further preprocessing

#### 4.2.1 Preprocessing and Analysis

Figure 4.1 shows the co-registration of the mean fMRI images over the newly created subject-specific atlas, taking into account the 62 neocortical labels from the Desikan atlas. This implies the use of real space for carrying out our research. We then checked for the overall distribution of correlation values of all the subjects in real space, as seen in figure 4.2, which shows a slightly right-skewed tail<sup>3</sup> signifying that most of the data is clustered on the left to center scale.

We also found a similar right-skewed tail for each subject in both the real space(B.2) and MNI representation of the brain, with a slight difference in the mean and standard deviation. An example of the trend can be seen in figure 4.3, which shows the correlation matrix for subject 1 along with the distribution of the occurrences of the correlation values.

As the difference between the adjacency matrices of each subject is so minimal, we decided to take the difference between the mean of the vulnerable group and the mean of the resilient group for further analysis, which is shown in figure 3.2. These were then used by our Machine Learning models for further analysis.

#### 4.2.2 Statistical Inference

We analyzed the mean group differences between the adjacency matrices of the vulnerable and the resilient groups and then used the absolute values to rank the connections. The result is described in table 4.3.

<sup>&</sup>lt;sup>3</sup>https://www.expii.com/t/normal-distribution-right-and-left-skewed-graphs-5338

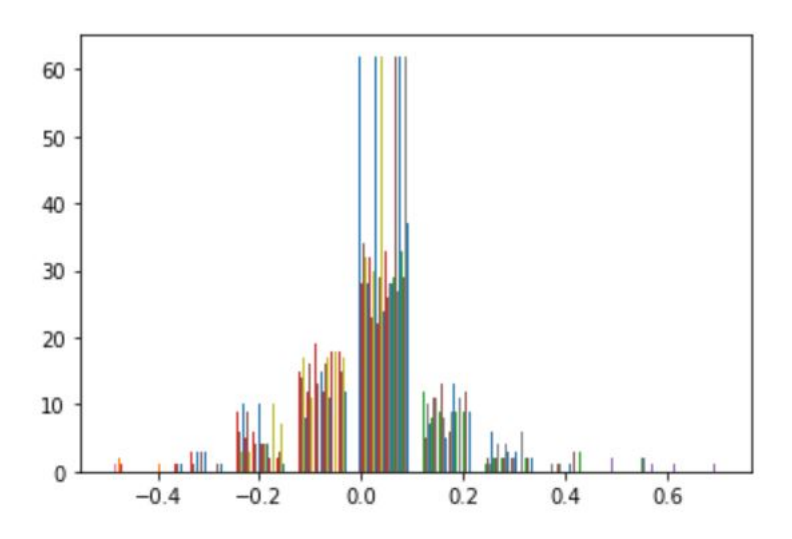


**Figure 4.2:** Overall distribution of correlation values of all the subjects in real space, clearly indicating a normal distribution with a mean of little over 0.

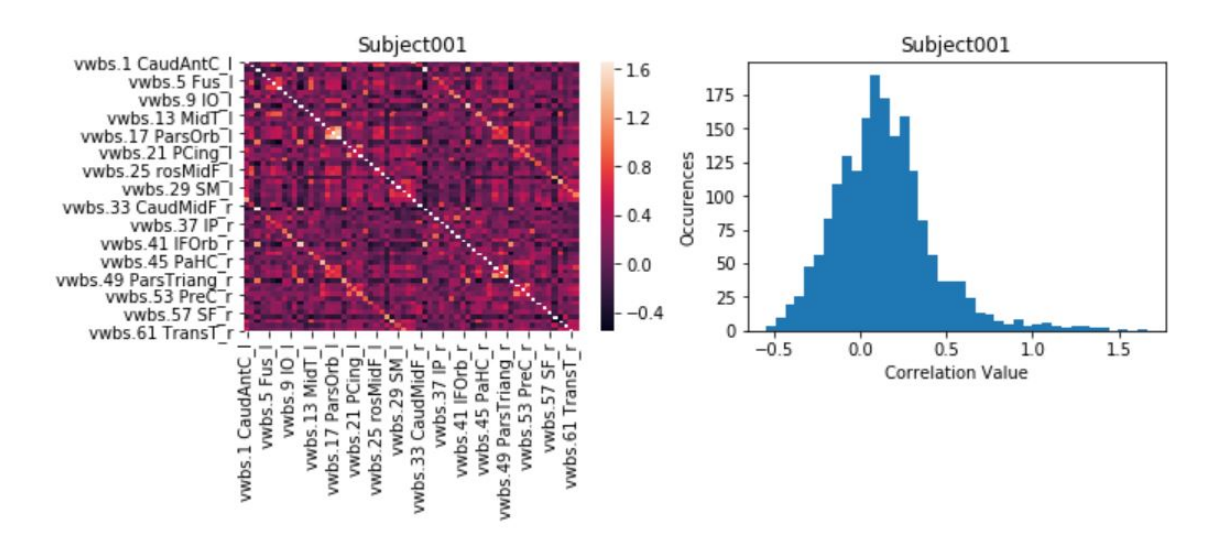


**Figure 4.3:** Correlation map of subject 1 on the left hand side showing the same region values in the center and the upper and lower diagonal showing the left and right hemispheres of the brain, and distribution of correlation values on the right side with a right tailed distribution.

Group Difference - Stats. Inference	
Pars Opercularis left, Rostral Middle Frontal right	
Pericalcarine right, Superior Temporal right	
Pars Opercularis right, Rostral Middle Frontal left	
Superior Temporal left, Pericalcarine right	
Pericalcarine left, Superior Temporal right	0.22
Caudal Anterior Cingulate right, Superior Frontal right	0.22
Cuneus left, Pericalcarine left	
Posterior Cingulate right, Superior Frontal left	
Pars Triangularis right, Rostral Middle Frontal left	
Pars Opercularis left, Caudal Anterior Cingulate right	

**Table 4.3:** Rankings of important connects from mean group differences between connections

#### 4.2.3 Baseline Model

We started our experimentation by creating baseline linear models, namely Linear Regression, Logistic Regression, and Support Vector Machines. The features are ranked based on the model coefficients from the linear models and will be compared with our experimented models.

The linear models have been fitted 100 times by selecting different sets of random subjects based on 70%-30% split, resulting in separate features responsible for the resilience and separate classification scores ( $R^2$  coefficient for linear models). We then managed to select the top 10 connections from the linear models, based on how many times each connection appears in the top-10 feature list for various models. For the Logistic Regression, we have managed an average accuracy of 58%, and for the Support Vector Machine, we managed an average accuracy of 60%. The important connections from the Linear Regression can be seen in table 4.2, the important connections from the Logistic Regression can be seen in table 4.2 and the important connections from the Support Vector Machine can be seen in table 4.2.

We also created an adjacency matrix comparison amongst the connections responsible for resilience amongst the three linear models, which can be seen in figure 4.4.

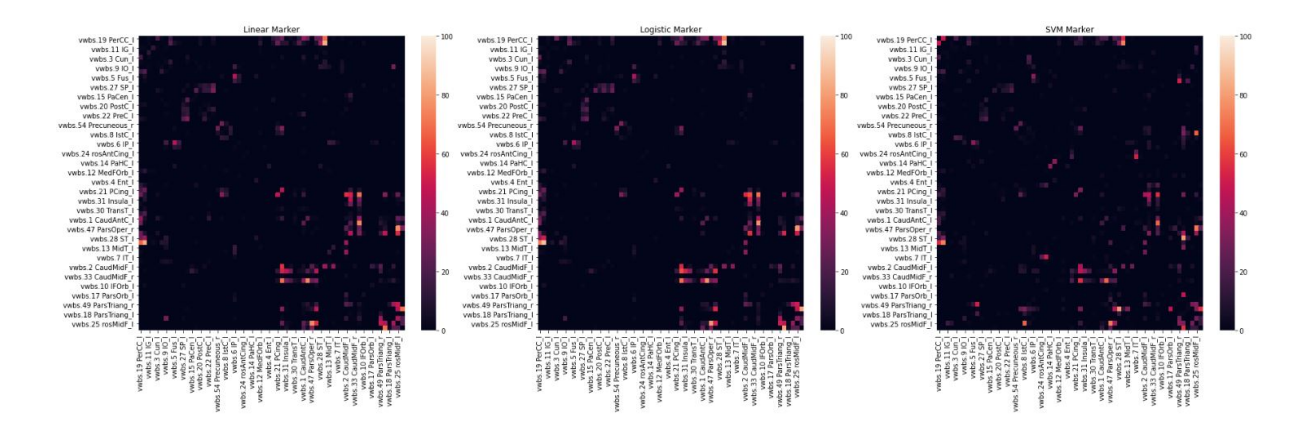


**Figure 4.4:** Connections of Resilience in matrix form from the 3 linear models, with Linear Regression in the left, Logistic Regression in the middle, and Support Vector Machine on the right.

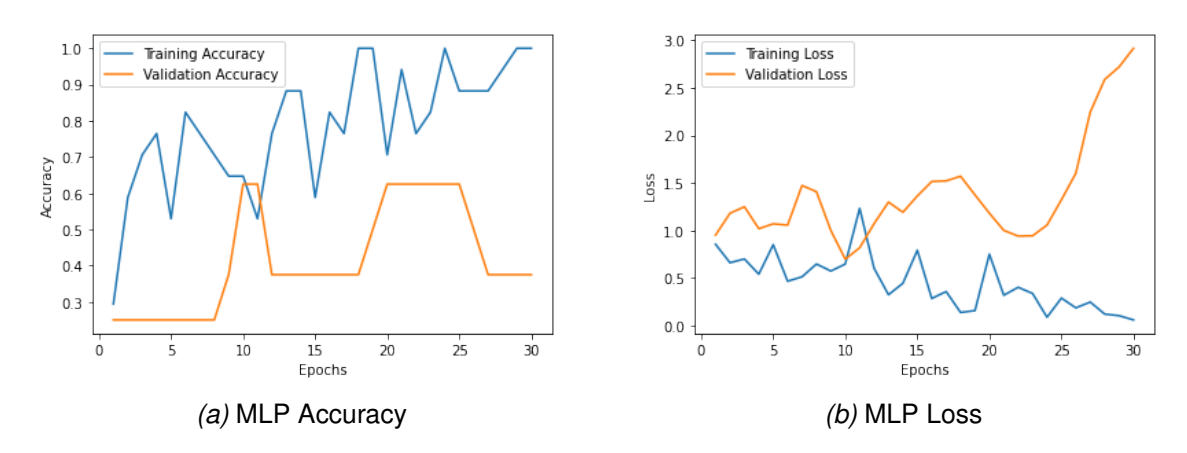
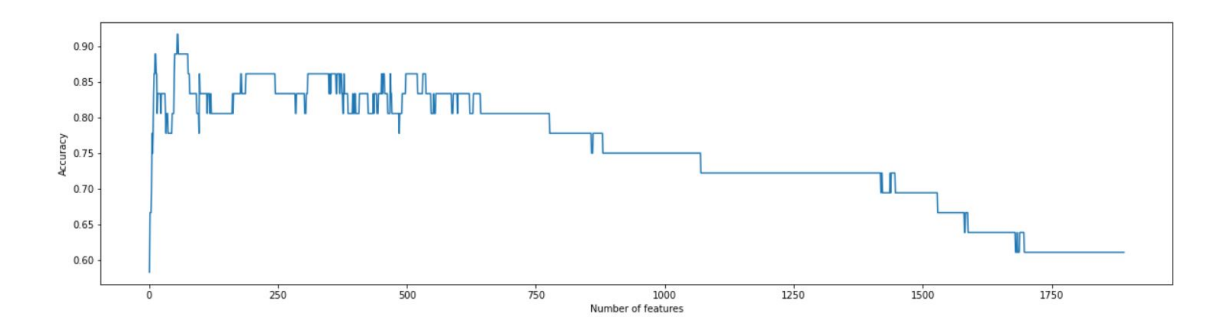


Figure 4.5: Training Accuracy and Loss for initial MLP model

### 4.2.4 Multi-layer Perceptron

#### **Model Training and Testing**

After the baseline linear models, the next step of our experiment was to train our data on a multi-layer perceptron. Even before training, there was an expectation of overfitting the data as the number of features (connections) was too high as compared to the number of subjects. Training an initial model on the entire dataset for around 30 epochs gave us an average training accuracy of 97%, average validation accuracy of 57%, and average testing accuracy of 60% with a standard deviation of around 10%, as seen in figure 4.8. This indicated overfitting of the data, and also the fact that the feature ordering might play a significant role in the classification accuracy. A dirty way I used to remove overfitting is by including a 100-fold MLP model where for each fold, we randomly select the subjects based on previously accepted 49%-21%-30% split. Each version of the created dataset then goes into



**Figure 4.6:** MLP Model on various number of features. On the Y-axis, we have the accuracies of different models and on the X-axis, we have the number of features.

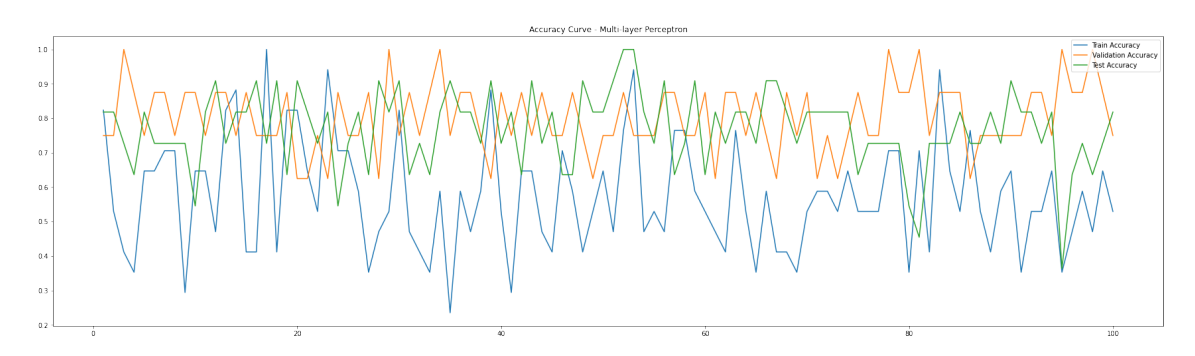


**Figure 4.7:** Our MLP model on various number of iterations. On the y-axis, we have the train, test and validation accuracy values and on the x-axis, we have the number of folds.

the MLP model 100 times based on a different sampling of the features. We treat each sampling as the ranking for the features, as we've seen from the figure 4.7 that after a certain number of features, the model fails to make more sense of the added features and the classification accuracy drops significantly to a chance. We trained our MLP based on the hyperparameters described in the previous section, which resulted in the graph below with an average training accuracy of 57.3%, average validation accuracy of 51.25% and an average test accuracy of 61.81%.

#### 4.2.5 BrainGNN

The dataset was divided into 49%-21%-30% split after trying out a series of different folds, where the fold mentioned above performed the best. We devised the dataset 100 times, running the model for each iteration, selecting the best model for testing, and recording the scores. The average accuracy and loss plots are shown in 4.8.

The final average train accuracy was recorded at 72%, validation accuracy was recorded at 20% and test accuracy was recorded to be 62%.

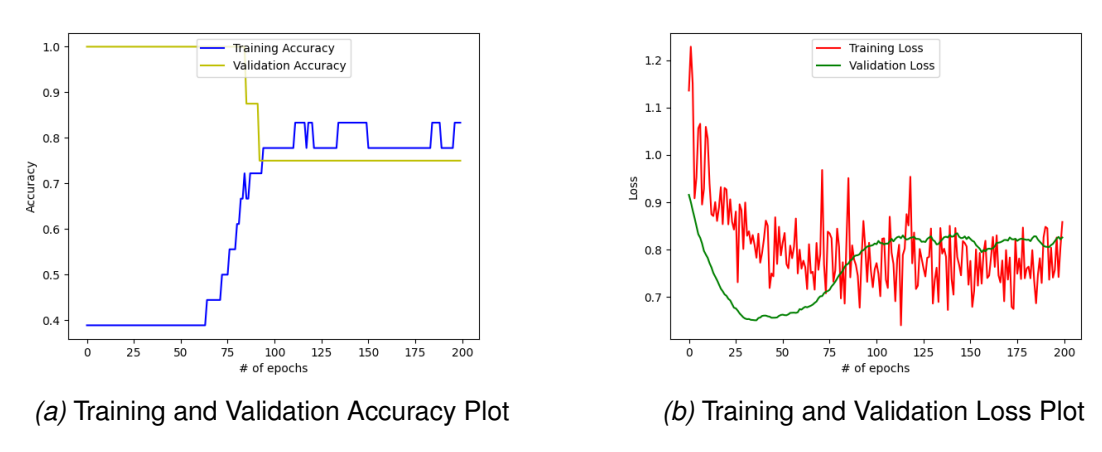


Figure 4.8: BrainGNN Training/Validation Accuracy/Loss Plot

Even though the validation dataset was too low to get any significant result, I believe the result is far off from being clear-cut. However, we decided to keep the top-10 regions of interest in place of the most number of ROIs presented in the top-10 most of the time, as seen in table 4.2.

#### 4.2.6 Feature Engineered Neural Network

We decided to use 100 different model coefficients fitted each time after dividing the dataset into a 70%-30% split randomly, ranking the absolute model coefficient, effectively understanding the top features (connections). We then selected the top 30 connections from this ranked list, then divided the dataset into our selected 49%-21%-30% train-validation-test split, sampled the features randomly 100 times, and sent them to the Multi-layer Perceptron model for training and testing. This gave us an average training accuracy of 72%, average validation accuracy of 65%, and an average testing accuracy of 64%. I also recorded the top-10 connections, which were ranked in the top-10 most of the time in the loop, hereby confirming biomarkers of stress resilience. The result is shown in table 4.2.

### 4.2.7 Final Ranking and Prediction

A comparison has been drawn between all the machine learning models to find robust biomarkers of stress resilience. We found that 6 out of the top 10-ranked connections stood out from all the machine learning models, effectively saying that those connections are robust to different settings. The rankings can be seen in table 4.4.

Pericalcarine Right - Superior Temporal Right	
Pars Opercularis Left - Rostral Middle Frontal Right	
Rostral Middle Frontal left - Pars Opercularis Right	
Caudal Anterior Cingulate Right - Superior Frontal Right	
Pericalcarine Left - Superior Temporal Right	
Posterior Cingulate Right - Superior Frontal Right	

Table 4.4: Robust biomarkers from all machine learning models

Subject	Prediction
Subject008	Vulnerable
Subject037	Vulnerable
Subject038	Vulnerable
Subject039	Vulnerable
Subject041	Resilient
Subject042	Resilient
Subject044	Vulnerable
Subject045	Resilient
Subject046	Vulnerable

**Table 4.5:** Predictions of healthy control subjects based on feature-engineered Multi-layer Perceptron

We also had 9 healthy control subjects who were not exposed to any sort of stress. We made predictions for the said subjects, as to which group they might fall into based on our feature-engineered multi-layer perceptron. The predictions are shown in table 4.5.

Kinser et. al. [52] states that almost 80% of the people in the world are more susceptible to stress, and end up having some forms of mental issues if exposed to it. Our analysis shows that almost 67% of the people in the population data shared by Leiden Medical Center belong to the vulnerable category.

# **Chapter 5**

### Conclusion

In our thesis, we sought to investigate stress resilience using resting-state fMRI brain imaging, thereby assisting us in better understanding the impact of stress on the brain and the possibility of identifying biomarkers of stress resistance.

We present two ways that helped us to converge on biomarkers of stress resilience. We first introduce statistical inferences, which can be used to find biomarkers by analyzing the group differences between the resilient and vulnerable groups of people. The second way is by using different Machine Learning models to analyze the connections and converging on biomarkers of stress resilience with good accuracy.

We have analyzed the connections using several Machine Learning models, including Linear Models, Neural networks, and state-of-the-art BrainGNN, which is a highly interpretable Brain Graph Neural Network for fMRI analysis. However, due to the unavailability of much data, we didn't manage to get robust ROIs and faced the problem of overfitting. This allowed us to research alternate solutions that would avoid the low data problem.

We introduced a novel framework for our research, called the feature-engineered Multi-layer Perceptron, which takes in the most important features based on model coefficients from linear models, and they're trained effectively with the help of a multi-layer perceptron to provide better classification accuracy and robust biomarkers of stress resilience.

### 5.1 Limitations of study

The frameworks presented in this thesis come with their limitations as well. The biggest limitation to our research is the availability of data, as it is in the case of

much medical research. This led to another major limitation, which has been the absence of an end-to-end evaluation for our proposed feature-engineered multi-layer perceptron framework that would require lots of resources and data to train the different classifiers and make them order-independent for ranking. Another limitation, coming from the low data availability, was in the case of reduction of data dimensionality. We reduced the brain ROIs from 92 to 62, which led to a lot of ROIs being merged, effectively biasing the data to a few clusters, and hindering us from finding robust biomarkers.

### **5.2 Future Prospects**

Several directions could effectively advance the research on stress resilience. I have listed the following that I believe would advance the research by a considerable amount:

- We could employ more robust statistical analysis like clustering, and grouping based on connections, effectively trying to understand whether some clusters play a better role in resilience as compared to others.
- If we have enough data, we could try out various state-of-the-art Graph Neural Network models to understand the network connections within the brain and get better classification results.
- If we have enough data, we also don't reduce the data dimensionality considerably, as was the case for clustering some of the brain regions from 92 ROIs to 62 ROIs.
- We could also enhance the fe-MLP framework by ranking the initial features based on a combination of the linear models, and then using the subsequent rankings in more complicated neural networks, to get better classification scores, and hence, better biomarkers of stress resilience.

# **Bibliography**

- [1] L. D. Godoy, M. T. Rossignoli, P. Delfino-Pereira, N. Garcia-Cairasco, and E. H. de Lima Umeoka, "A comprehensive overview on stress neurobiology: Basic concepts and clinical implications," Frontiers in Behavioral Neuroscience, vol. 12, p. 127, 2018. [Online]. Available: https://www.frontiersin.org/article/10.3389/fnbeh.2018.00127
- [2] A. Nieto-Castanon, Handbook of functional connectivity Magnetic Resonance Imaging methods in CONN, 02 2020.
- [3] X. Li, Y. Zhou, S. Gao, N. Dvornek, M. Zhang, J. Zhuang, S. Gu, D. Scheinost, L. Staib, P. Ventola, and J. Duncan, "BrainGNN: Interpretable brain graph neural network for fmri analysis," bioRxiv, 2020. [Online]. Available: https://www.biorxiv.org/content/early/2020/05/22/2020.05.16.100057
- [4] T. C. Kietzmann, P. McClure, and N. Kriegeskorte, "Deep neural networks in computational neuroscience," *bioRxiv*, 2018. [Online]. Available: https://www.biorxiv.org/content/early/2018/06/05/133504
- [5] P. M. Matthews and P. Jezzard, "Functional magnetic resonance imaging," *Journal of Neurology, Neurosurgery & Psychiatry*, vol. 75, no. 1, pp. 6–12, 2004. [Online]. Available: https://jnnp.bmj.com/content/75/1/6
- [6] N. Schneiderman, G. Ironson, and S. D. Siegel, "Stress and health: Psychological, behavioral, and biological determinants," *Annual Review of Clinical Psychology*, vol. 1, no. 1, pp. 607–628, 2005, pMID: 17716101. [Online]. Available: https://doi.org/10.1146/annurev.clinpsy.1.102803.144141
- [7] S. N. Setroikromo, S. E. Bauduin, J. E. Reesen, S. J. van der Werff, A. S. Smit, E. Vermetten, and N. J. van der Wee, "Cortical Thickness in Dutch Police Officers: An Examination of Factors Associated with Resilience," *Journal of Traumatic Stress*, vol. 33, no. 2, pp. 181–189, 2020. [Online]. Available: https://onlinelibrary.wiley.com/doi/abs/10.1002/jts.22494

[8] M. Skogstad, M. Skorstad, A. Lie, H. S. Conradi, T. Heir, and L. Weisæth, "Work-related post-traumatic stress disorder," *Occupational Medicine*, vol. 63, no. 3, pp. 175–182, 03 2013. [Online]. Available: https://doi.org/10.1093/occmed/kqt003

- [9] G. Glover, "Overview of functional magnetic resonance imaging," *Neurosurgery clinics of North America*, vol. 22, pp. 133–9, vii, 04 2011.
- [10] D. Georgetown, "What is neuroscience?" pp. 1038 1049, 2020.
- [11] M. W. Voss, L. S. Nagamatsu, T. Liu-Ambrose, and A. F. Kramer, "Exercise, brain, and cognition across the life span," *Journal of Applied Physiology*, vol. 111, no. 5, pp. 1505–1513, 2011, pMID: 21527670. [Online]. Available: https://doi.org/10.1152/japplphysiol.00210.2011
- [12] M. Baratta, R. Rozeske, and S. Maier, "Understanding stress resilience," *Frontiers in behavioral neuroscience*, vol. 7, p. 158, 11 2013.
- [13] G. Wu, A. Feder, H. Cohen, J. Kim, S. Calderon, D. Charney, and A. Mathé, "Understanding resilience," *Frontiers in behavioral neuroscience*, vol. 7, p. 10, 02 2013.
- [14] S. Van der Werff, S. van den Berg, J. N. Pannekoek, B. Elzinga, and N. Wee, "Neuroimaging resilience to stress: A review," *Frontiers in behavioral neuro-science*, vol. 7, p. 39, 05 2013.
- [15] S. J. A. van der Werff, J. N. Pannekoek, D. J. Stein, and N. J. A. van der Wee, "Neuroimaging of resilience to stress: current state of affairs," *Human Psychopharmacology: Clinical and Experimental*, vol. 28, no. 5, pp. 529–532, 2013. [Online]. Available: https://onlinelibrary.wiley.com/doi/abs/10.1002/hup. 2336
- [16] B. Fischl and A. M. Dale, "Measuring the thickness of the human cerebral cortex from magnetic resonance images," *Proceedings of the National Academy of Sciences*, vol. 97, no. 20, pp. 11050–11055, 2000. [Online]. Available: https://www.pnas.org/content/97/20/11050
- [17] K. Slaney, M. Tkatchouk, S. Gabriel, and M. Maraun, "Psychometric assessment and reporting practices: Incongruence between theory and practice," *Journal of Psychoeducational Assessment J PSYCHOEDUC ASSESS*, vol. 27, pp. 465–476, 11 2009.

[18] H. Huang and M. Ding, "Linking functional connectivity and structural connectivity quantitatively: A comparison of methods," *Brain Connectivity*, vol. 6, 11 2015.

- [19] D. A. Raichlen, P. K. Bharadwaj, M. C. Fitzhugh, K. A. Haws, G.-A. Torre, T. P. Trouard, and G. E. Alexander, "Differences in resting state functional connectivity between young adult endurance athletes and healthy controls," *Frontiers in Human Neuroscience*, vol. 10, p. 610, 2016. [Online]. Available: https://www.frontiersin.org/article/10.3389/fnhum.2016.00610
- [20] S. Whitfield-Gabrieli and A. Nieto-Castanon, "Conn: A functional connectivity toolbox for correlated and anticorrelated brain networks," *Brain Connectivity*, vol. 2, pp. 125–41, 05 2012.
- [21] Y. Behzadi, K. Restom, J. Liau, and T. Liu, "Behzadi y, restom k, liau j, liu tt. a component based noise correction method (compcor) for bold and perfusion based fmri. neuroimage 37: 90-101," *NeuroImage*, vol. 37, pp. 90–101, 09 2007.
- [22] H. Huang and Y. Sun, "Visualization and assessment of spatio-temporal covariance properties," *Spatial Statistics*, vol. 34, p. 100272, 2019, spatio-temporal and geostatistical analysis of hydrological events and related hazards. [Online]. Available: https://www.sciencedirect.com/science/article/pii/S2211675317301306
- [23] N. Logothetis, "Logothetis nk. the neural basis of the blood-oxygen-level-dependent functional magnetic resonance imaging signal. philos trans r soc lond b biol sci 357: 1003-1037," *Philosophical transactions of the Royal Society of London. Series B, Biological sciences*, vol. 357, pp. 1003–37, 09 2002.
- [24] D. Cordes, V. Haughton, K. Arfanakis, G. Wendt, P. Turski, C. Moritz, M. Quigley, and M. Meyerand, "Mapping functionally related regions of brain with functional connectivity mri (fcmri)," *AJNR. American journal of neuroradiology*, vol. 21, pp. 1636–44, 11 2000.
- [25] B. S. Aribisala, J. He, and A. Blamire, "Comparative study of standard space and real space analysis of quantitative mr brain data," *Journal of Magnetic Resonance Imaging*, vol. 33, 2011.
- [26] J. Zhu, Y. Xu, L. Hoegner, and U. Stilla, "Direct co-registration of tir images and mls point clouds by corresponding keypoints," *ISPRS Annals of Photogrammetry, Remote Sensing and Spatial Information Sciences*, vol. IV-2/W7, pp. 235–242, 09 2019.

[27] X. Yang, R. Kwitt, M. Styner, and M. Niethammer, "Quicksilver: Fast predictive image registration - a deep learning approach," *NeuroImage*, vol. 158, 03 2017.

- [28] A. F. Filippi M, Cividini C, "Deep learning: a turning point in acute neurology," *Lancet Digit Health*, 2020, pMID: 33328119.
- [29] A. Dalmia, G. Jawahar, and M. Gupta, "Towards interpretation of node embeddings," 04 2018, pp. 945–952.
- [30] J. Zhou, G. Cui, Z. Zhang, C. Yang, Z. Liu, and M. Sun, "Graph neural networks: A review of methods and applications," *ArXiv*, vol. abs/1812.08434, 2018.
- [31] Y. Munakata and J. Mcclelland, "Connectionist models of development," *Developmental Science*, vol. 6, pp. 413 429, 09 2003.
- [32] J. Kawahara, C. J. Brown, S. P. Miller, B. G. Booth, V. Chau, R. E. Grunau, J. G. Zwicker, and G. Hamarneh, "BrainNetCNN: Convolutional neural networks for brain networks; towards predicting neurodevelopment," NeuroImage, vol. 146, pp. 1038 – 1049, 2017. [Online]. Available: http://www.sciencedirect.com/science/article/pii/S1053811916305237
- [33] K. O'Shea and R. Nash, "An introduction to convolutional neural networks," ArXiv e-prints, 11 2015.
- [34] S. Mondello, M. M. Salama, W. M. Y. Mohamed, and F. H. Kobeissy, "Editorial: Biomarkers in neurology," *Frontiers in Neurology*, vol. 11, p. 190, 2020. [Online]. Available: https://www.frontiersin.org/article/10.3389/fneur.2020.00190
- [35] H. Gao and S. Ji, "Graph u-nets," 2019.
- [36] B. Alexander, W. Loh, L. Matthews, A. Murray, C. Adamson, R. Beare, J. Chen, C. Kelly, P. Anderson, L. Doyle, A. Spittle, J. Cheong, M. Seal, and D. Thompson, "Desikan-killiany-tourville atlas compatible version of m-crib neonatal parcellated whole brain atlas: The m-crib 2.0," *Frontiers in Neuroscience*, vol. 13, 02 2019.
- [37] T. Briand and P. Monasse, "Theory and practice of image b-spline interpolation," Image Processing On Line, vol. 8, pp. 99–141, 07 2018.
- [38] D. B. Parker and Q. R. Razlighi, "The benefit of slice timing correction in common fmri preprocessing pipelines," *Frontiers in Neuroscience*, vol. 13, p. 821, 2019. [Online]. Available: https://www.frontiersin.org/article/10.3389/fnins. 2019.00821

[39] R. Sladky, K. J. Friston, J. Tröstl, R. Cunnington, E. Moser, and C. Windischberger, "Slice-timing effects and their correction in functional mri," *NeuroImage*, vol. 58, no. 2, pp. 588 – 594, 2011. [Online]. Available: http://www.sciencedirect.com/science/article/pii/S1053811911007245

- [40] J. Ashburner and K. Friston, "Unified segmentation," *NeuroImage*, vol. 26, pp. 839–51, 08 2005.
- [41] J. Chen, A. MacEachren, and D. Peuquet, "Constructing overview + detail dendrogram-matrix views," *IEEE transactions on visualization and computer graphics*, vol. 15, pp. 889–96, 01 2010.
- [42] S. Luthar, "Vulnerability and resilience: A study of high-risk adolescents," *Child Development*, vol. 62, pp. 600 616, 06 1991.
- [43] G. Huang, Z. Liu, L. van der Maaten, and K. Q. Weinberger, "Densely connected convolutional networks," 2018.
- [44] N. Srivastava, G. Hinton, A. Krizhevsky, I. Sutskever, and R. Salakhutdinov, "Dropout: A simple way to prevent neural networks from overfitting," *J. Mach. Learn. Res.*, vol. 15, no. 1, p. 1929–1958, Jan. 2014.
- [45] A. F. Agarap, "Deep learning using rectified linear units (relu)," 2019.
- [46] C. Nwankpa, W. Ijomah, A. Gachagan, and S. Marshall, "Activation functions: Comparison of trends in practice and research for deep learning," 2018.
- [47] D. P. Kingma and J. Ba, "Adam: A method for stochastic optimization," 2017.
- [48] X. Li, Y. Zhou, N. C. Dvornek, M. Zhang, J. Zhuang, P. Ventola, and J. S. Duncan, "Pooling regularized graph neural network for fmri biomarker analysis," 2020.
- [49] X. Li, N. C. Dvornek, Y. Zhou, J. Zhuang, P. Ventola, and J. S. Duncan, "Graph neural network for interpreting task-fmri biomarkers," 2019.
- [50] C. Cangea, P. Veličković, N. Jovanović, T. Kipf, and P. Liò, "Towards sparse hierarchical graph classifiers," 2018.
- [51] B. Knyazev, G. W. Taylor, and M. R. Amer, "Understanding attention and generalization in graph neural networks," 2019.
- [52] P. A. Kinser and D. E. Lyon, "A conceptual framework of stress vulnerability, depression, and health outcomes in women: potential uses in research on complementary therapies for depression," *Brain*

and Behavior, vol. 4, no. 5, pp. 665–674, 2014. [Online]. Available: https://onlinelibrary.wiley.com/doi/abs/10.1002/brb3.249

# **Appendix A**

# **Machine Learning**

#### A.1 Artificial Neural Network

The term "Artificial Neural Network" is derived from biological neural networks, which are responsible for the development of the human brain's structure. Artificial neural networks, like the real brain, have neurons that are connected at several levels. Nodes are the collective term for these neurons. The dendrites from biological neural networks represent inputs, the cell nucleus represents nodes, the synapse represents weights, and the axon represents output in Artificial Neural Networks. The biological neuron is depicted in figure A.1, while the artificial neuron is depicted in figure A.2.

To grasp the concept of the architecture of an artificial neural network, we must first understand what a neural network is. A neural network is defined by the placement of a large number of artificial neurons, referred to as units, in a succession of layers. Consider the numerous layers that can be found in an artificial neural network. The three levels of an Artificial Neural Network are as follows:

• Input Layer: This layer takes in inputs from the user.

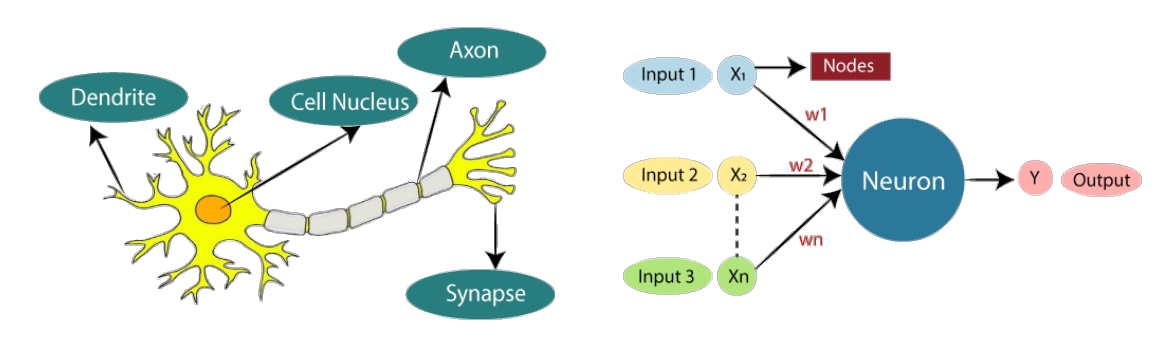


Figure A.2: A classic example of Artificial

Figure A.1: A classic example of Biological neuron

neuron

- **Hidden Layer**: Between the input and output layers is a hidden layer. It performs all of the mathematics necessary to unearth hidden traits and patterns.
- **Output Layer**: The hidden layer modifies the input and communicates the outcome via this layer. When an input is received, the artificial neural network calculates both the weighted sum of the inputs and the bias. A transfer function is used to express this computation.

$$\sum_{i=1}^{n} w_i * X_i + b$$

It computes the weighted sum, which is then passed to an activation function to get the outcome. Activation functions control whether a node should fire or not. Only those who are fired make it to the output layer. There are a variety of activation functions accessible, depending on the type of work being performed.

The best way to think of an Artificial Neural Network is as a weighted directed graph with artificial neurons serving as nodes. Directed edges with weights can be used to depict the relationship between neuron outputs and neuron inputs. An external source provides an Artificial Neural Network with an input signal in the form of a pattern and a picture in the form of a vector. Following that, these inputs are mathematically assigned using the notation x(n) for each of the n inputs.

Then, each input is multiplied by the weights associated with it (these weights are the details utilized by artificial neural networks to solve a specific problem). These weights, in general, describe the strength of the connections between neurons inside an artificial neural network. Within each computing unit, all weighted inputs are added.

If the weighted sum equals zero, either bias is applied to the output to make it non-zero, or another method is employed to scale up to the system's response. The inputs for bias and weight are identical, and weight equals one. The sum of weighted inputs can be any value between 0 and positive infinity in this scenario. To ensure that the response remains within acceptable bounds, a specified maximum value is bench-marked and the sum of weighted inputs is routed via the activation function.

Activation function is a group of transfer functions that work cooperatively to achieve the desired effect. While activation functions can take on any shape or size, they are frequently composed of linear or non-linear sets of functions. As seen in figure A.3

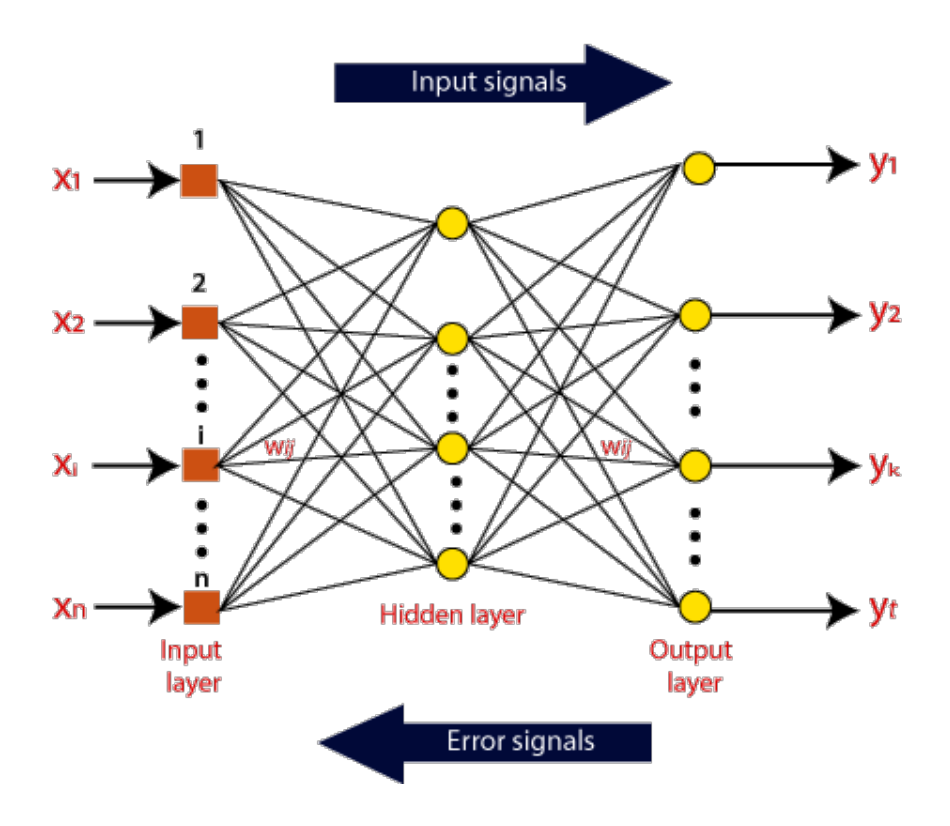


Figure A.3: Working of an artificial neural network

and extensively explored in the article ANN <sup>1</sup>, the binary, linear, and tan hyperbolic sigmoidal activation functions are among the most commonly used sets of activation functions.

### A.2 Overfitting, underfitting, & bias-variance tradeoff

The ideas of overfitting, underfitting, and the bias-variance tradeoff are all crucial to machine learning. Overfitting occurs when a model's performance on the training data used to fit the model is much better than its performance on a test set that was not included in the model training process. For example, the prediction error for training data may be considerably smaller than that for testing data. One of the key reasons for separating data for training and testing is to enable the comparison of model performance measures across these two data sets. This enables the model's forecasting capability to be validated using new, previously unseen data.

A model is said to have a large variance if it overfits the training data. One way to look at it is that whatever variability there is in the training data, the model has done an excellent job of "learning" it. It is far too accurate. A model with a large

<sup>&</sup>lt;sup>1</sup>https://www.javatpoint.com/artificial-neural-network

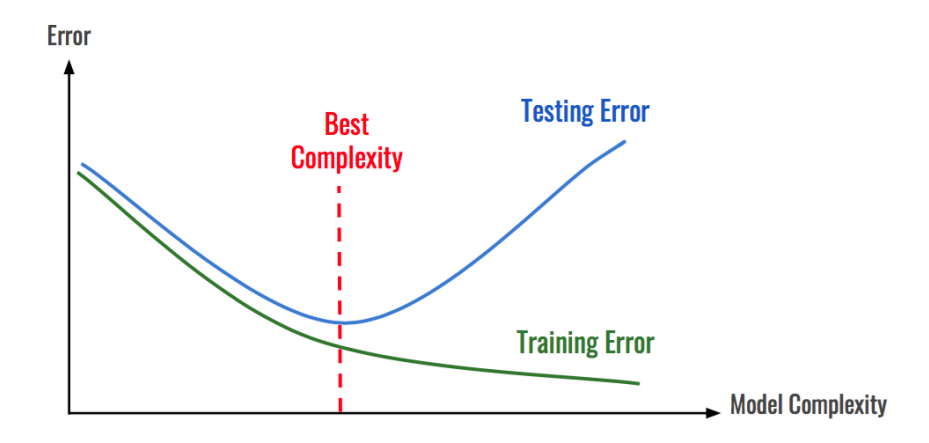


Figure A.4: Bias Variance Tradeoff

variance has almost certainly learned how to deal with noise in the training data. The term "noise" refers to random fluctuations, or deviations from true values, in the characteristics (independent variables) and responsiveness of data (dependent variable). Noise can conceal the true relationship between features and the response variable. Almost all the data in the current world is noisy.

If the training set contains random noise, the test set almost certainly contains random noise as well. Due to the unpredictable nature of the noise, the random fluctuations' specific values will differ from those of the training set. The model is unable to predict oscillations in the new, previously unreported data in the testing set. This is why the testing performance of an overfitted model is worse than its training performance.

Overfitting is more likely in the following circumstances:

- There are a considerable number of possible features in comparison to the number of samples (observations).
- The more features there are, the more likely it is that an erroneous association between the features and the response will be discovered.

In complex models, deep decision trees or neural networks are used. These types of models generate their features effectively and have the ability to establish more sophisticated assumptions about the link between characteristics and response, increasing the likelihood of overfitting. On the other hand, if a model does not closely match the training data, this is referred to as underfitting, and the model is deemed biased. In this case, the model's properties or the type of model used may be overly simplistic. The trade-off between them is illustrated in figure A.4.

# **Appendix B**

# **Preprocessing Pipeline**

This section will be used to understand some of the nuances of the preprocessing pipeline, which are already mentioned in the aforementioned sections.

### **B.1** Importance of Normalization

The importance of normalization during fMRI preprocessing is as follows:

- This is necessary for the analysis of fMRI data at the between-subject level.
- To transform the brain images of each individual to reduce the variability between individuals and allow meaningful group analyses to be successfully performed.
- Improve the statistical power of the analysis.
- Increase generalizability of findings at the population level.
- Allows for cross-study comparisons.

### **B.2** MNI Space and Real space

Normally, in brain analysis, an individual's brain is registered in standard space (e.g., Talairach or MNI space)<sup>1</sup>, which normalizes differences in brain size and shape between participants. The MNI sought to define a more representational brain. In a two-stage procedure, they built a new template that was approximately matched to the Talairach brain. To begin, they analyzed 241 normal MRI scans manually, identifying a line extremely similar to the AC-PC line and the brain's margins. Each brain was sized to correspond to the Talairach atlas's comparable places. They next

<sup>&</sup>lt;sup>1</sup>https://brainmap.org/training/BrettTransform.html

utilized an automated nine-parameter linear technique to match 305 normal MRI images (all right-handed, 239 M, 66 F, age 23.4 +/-4.1) to the average of 241 brains matched to the Talairach atlas. They then developed an average of 305 brain scans altered in this manner-the MNI305. The MNI305 was the company's initial template. The current standard MNI template is the ICBM152, which is the average of 152 normal MRI scans matched to the MNI305 using a nine-parameter affine transform. This is the standard template used by the International Consortium for Brain Mapping; it is also the standard template used in SPM99.

An alternate method is to convert the standard space atlas-based ROI to the subject's space**real space** coordinate system. This latter method retains the ease of atlas-based analysis while keeping the integrity of the original picture data and is expected to exhibit less processing-related bias. This is the coordinate system used throughout the MRI scan, and so there should be no degradation in the picture or the associated ROIs for image analysis.

# **Appendix C**

# Visualization of biomarkers inside the brain

One of the major results from our Machine Learning models is the biomarkers of stress resilience. With the importance of the rankings, another very important aspect is the visualization of biomarkers inside the brain. Those visualizations give us a clear indication of which areas inside the brain is responsible for the resilience and provide a visual aspect for experts, which might help them in analyzing the results of the Machine Learning models. The visualizations are color-coded to show the different connections responsible for resilience. The visualizations can be seen in the following figures.

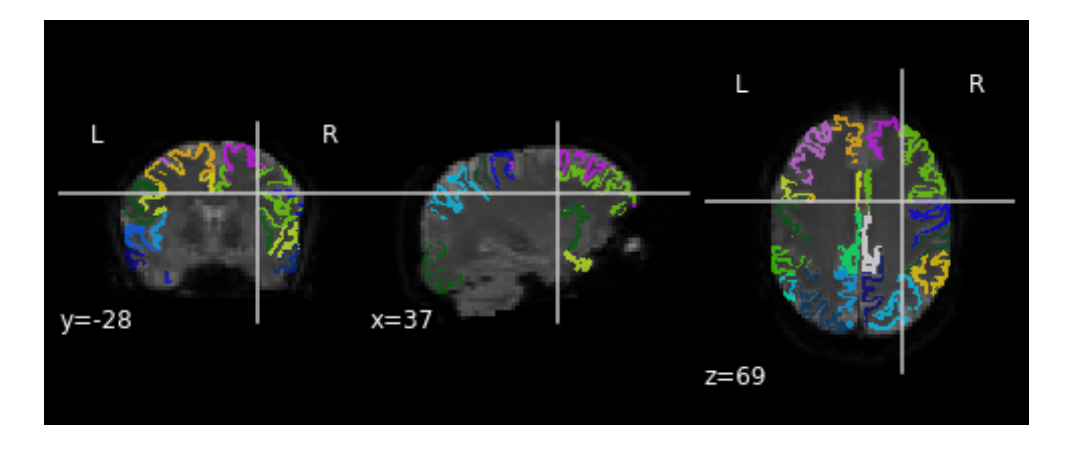


**Figure C.1:** Visualization of the biomarkers of stress resilience from Linear Regression model.

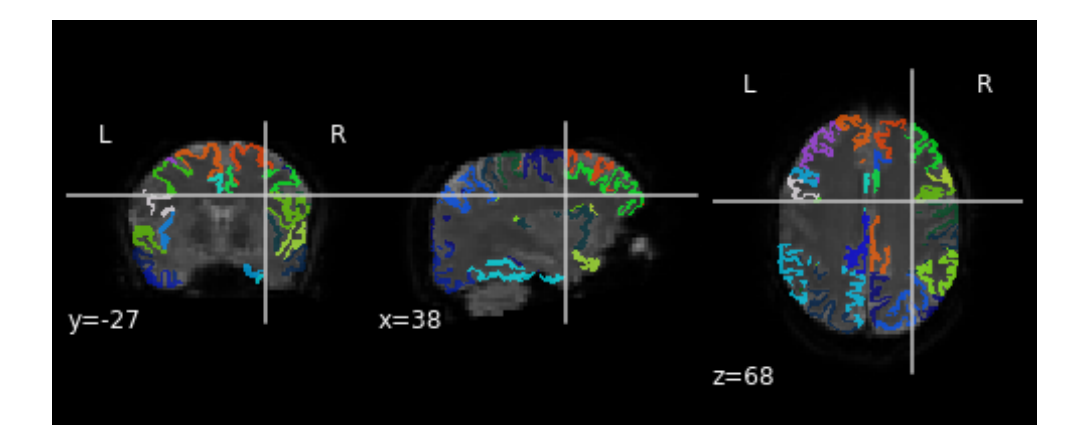


**Figure C.2:** Visualization of the biomarkers of stress resilience from Logistic Regression model.

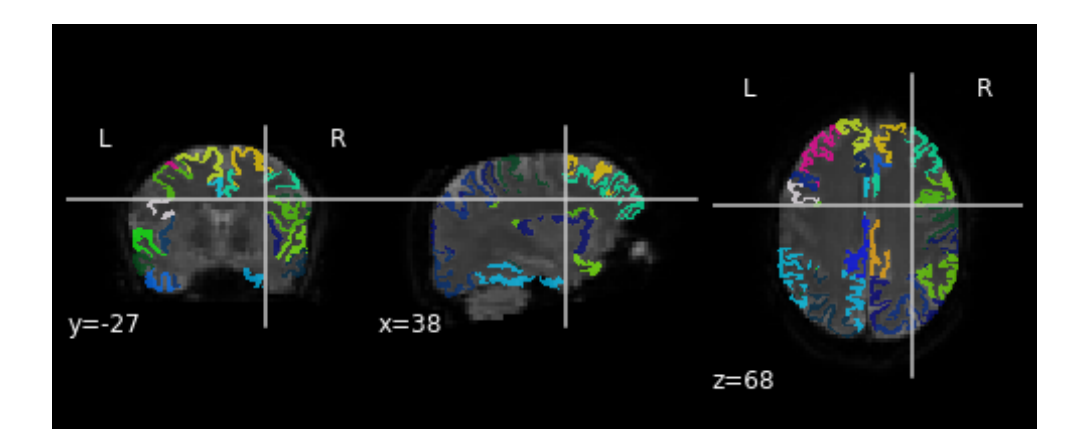


**Figure C.3:** Visualization of the biomarkers of stress resilience from Support Vector Machine model.

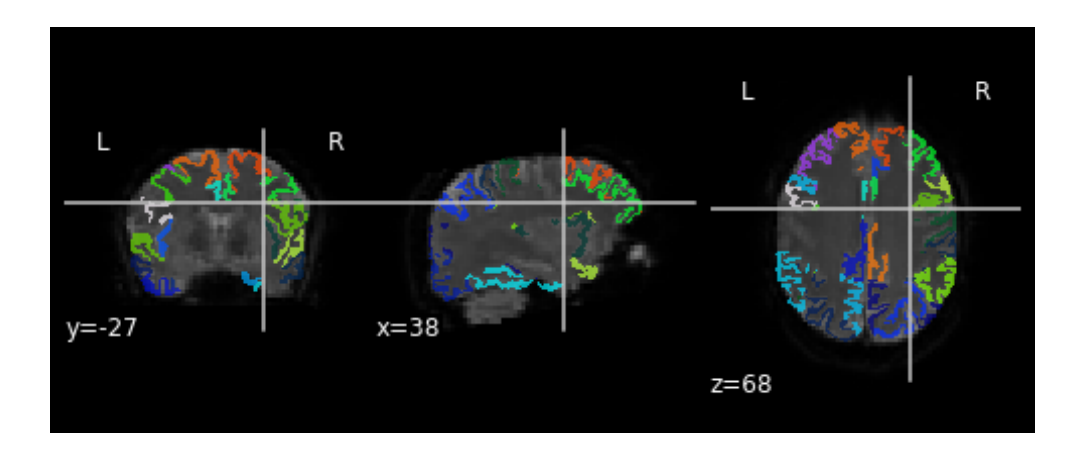


**Figure C.4:** Visualization of the biomarkers of stress resilience from Multi-layer Perceptron model.

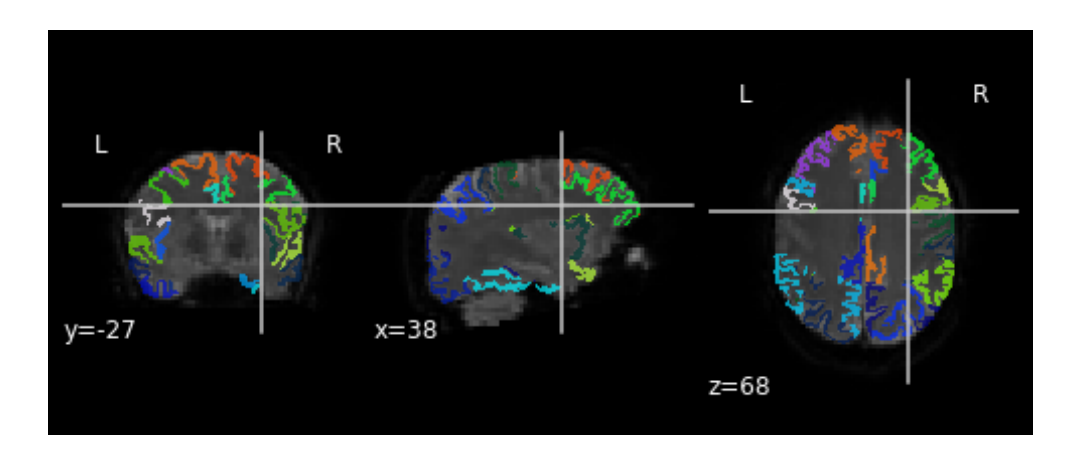


**Figure C.5:** Visualization of the biomarkers of stress resilience from feature-engineered Multi-layer Perceptron model.

# **Appendix D**

# **Mapping of ROIs to Brain Regions**

We have the following regions of interest from the brain, which have been in connection with the analysis, and the short to long-form has been mapped in this section in the following table. We have also used 'l' for 'left' and 'r' for 'right' in the aforementioned table, to show in which hemisphere of the brain does the ROI lies.

<b>Short Form</b>	Full form
CaudAntC	Caudal Anterior Cingulate
CaudMidF	Caudal Middle Frontal
Cun	Cuneus
Ent	Entorhinal
Fus	Fusiform
IP	Inferior Parietal
IT	Inferior Temporal
IstC	Isthmus Cingulate
LO	Lateral Occipital
LFOrb	Lateral Orbifrontal
LG	Lingual
MedFOrb	Medial Orbitofrontal
MidT	Middle Temporal
PaHC	Parahippocampal
PaCen	Paracentral
ParsOper	Pars Opercularis
ParsOrb	Pars Orbitalis
ParsTriang	Pars Triangularis
PerCC	Pericalcarine
PostC	Postcentral
PCing	Posterior Cingulate
PreC	Precentral
Precuneous	Precuneus
RosAntCing	Rostral Anterior Cingulate
RosMidF	Rostral Middle Frontal
SF	Superior Frontal
SP	Superior Parietal
ST	Superior Temporal
SM	Supramarginal
TransT	Transverse Temporal
Insula	Insula